

**DEVELOPMENT OF A RANDOM-FOREST-BASED MODEL FOR PREDICTING  
SLUG FLOW CHARACTERISTICS USING MACHINE LEARNING TECHNIQUE**

**BY**

**EBIRIM, Francis Onyema  
(M.ENG/SEET/2017/6739)**

**A THESIS SUBMITTED TO THE POSTGRADUATE SCHOOL, FEDERAL  
UNIVERSITY OF TECHNOLOGY, MINNA, NIGERIA IN PARTIAL  
FULFILLMENT OF THE REQUIREMENTS FOR THE AWARD OF THE  
DEGREE OF MASTER OF ENGINEERING IN CHEMICAL ENGINEERING**

**OCTOBER, 2021**

**ABSTRACT**

The development of heavy oil has attracted attention in recent times. With increasing fluid viscosity, slug flow has become the most common flow pattern in oil and gas pipeline flow which poses a challenge in flow assurance as the need for stability of system and production maximization. The accurate prediction of slug flow parameters is an urgent problem to be solved in heavy oil development for more efficiency in productivity. In this research paper, the analysis of experimental data for the Air-Silicon oil slug transition in a 67 mm diameter and 6 m long vertical pipe was carried out in this work. The superficial velocity ranges of gas and liquid obtained from the ECT were 0.047 – 4.727 m/s and 0.05 – 0.284 m/s respectively. This research makes use of Random-forest-based Machine learning technique to predict liquid hold up and slug flow regime characteristics at different time intervals due to as it uses random subspace method and bagging to prevent overfitting. From the investigated data, the liquid hold up, void fraction were obtained and other slug flow parameters obtained were; structural velocity, slug frequency, length of slug and film thickness. Comparison with the data from the proposed algorithm accurately predicts the liquid hold up, void fraction, and liquid film thickness. They were seen to have a good agreement with a Mean Square Error of 0.2 % with the Machine Learning based Random-forest prediction however slug frequency, structural velocity, and length of slug unit all had varying disagreement with the prediction leading to limitations in the use of the model algorithm in prediction of these flow parameters. The model was also tested against varying viscosity and a good agreement of over 99 % was seen from 5 cP to 1000 cP excluding high liquid viscosity of 5000 cP. The random-forest based machine learning model can then be used in predicting liquid hold up, void fraction, and liquid film thickness in low viscosity fluids less 1000 cP. The model developed aids the flow assurance and design involving multiphase flow slug flow in Oil and gas operations.

## TABLE OF CONTENTS

<b>Contents</b>	<b>Page</b>
Cover Page	
Title Page	i
Declaration	ii
Certification	Iii
Acknowledgements	Iv
Abstract	v
Table of Content	vi
List of Figures	x
<b>CHAPTER ONE</b>	
<b>1.0 INTRODUCTION</b>	1
1.1 Background of the Study	1
1.2 Statement of the Research Problem	2
1.3 Justification of the Study	2
1.4 Research Aim and Objectives	3
1.5 Scope of the Study	4
<b>CHAPTER TWO</b>	
<b>2.0 LITERATURE REVIEW</b>	5
2.2 Flow Regimes Classification in Two Phase Flows	6
2.2.1 Horizontal multiphase flow regimes in pipes	7
2.2.1.1 <i>Slug flow</i>	8

2.2.1.2 <i>Plug flow</i>	8
2.2.1.3 <i>Bubbly flow</i>	9
2.2.1.4 <i>Stratified flow</i>	9
2.2.1.5 <i>Stratified-wavy flow</i>	9
2.2.1.6 <i>Annular flow</i>	10
2.2.1.7 <i>Mist flow</i>	10
2.2.2 Vertical multiphase flow regimes in pipes	10
2.2.2.1 <i>Bubbly flow</i>	13
2.2.2.2 <i>Churn flow</i>	14
2.2.2.3 <i>Annular flow</i>	14
2.2.2.4 <i>Slug flow</i>	14
2.3 Slug Flow Characteristics	16
2.3.1 Rise velocity of taylor bubble	16
2.3.2 Models for liquid hold-up in vertical pipes	17
2.3.3 Slug frequency	22
2.3.4 Length of slug unit, taylor bubble and liquid slug	22
2.4 Parameters to Characterize Flow Regimes	24
2.4.1 Void fraction prediction in vertical pipe	24
2.4.2 Pressure drop prediction in vertical pipes	24
2.5 Models in Multiphase Flow	25
2.6 Machine Learning for Slug Flow Analysis	26
2.6.1 Python	27
2.6.1.1 <i>Why python for data science</i>	27

2.6.2 Artificial neural network (ANN) modelling	27
2.6.3 Computational fluid dynamics (CFD)	28
2.6.4 Neuro-fuzzy logic	28
2.7 Challenges in Machine Learning	29
2.8 Application of Machine Learning	30
2.9 Phase Distribution of an Air-Silicone Flow in a Vertical Pipe	31
2.10 Application of Vertical Multiphase Flow	33
<b>CHAPTER THREE</b>	<b>34</b>
<b>3.0 MATERIALS AND METHOD</b>	<b>34</b>
3.1 Data Acquisition	34
3.2 Analysis of Acquired Data	36
3.2.1 Model Generation and Validation	36
<b>CHAPTER FOUR</b>	<b>40</b>
<b>4.0 RESULTS AND DISCUSSION</b>	<b>40</b>
4.1 The Correlation of Simulated and Experimental Liquid Hold up ( $H_l$ ) and Void Fraction ( $V_f$ ) at Liquid Superficial Velocity ( $U_{sl}$ ) = 0.05 - 0.378 m/s	40
4.2 The Correlation of Simulated and Experimental Structural Velocity and Slug Frequency at ( $U_{sl}$ ) = 0.05 - 0.378 m/s	46
4.3 The Correlation of Simulated and Experimental Length of Slug Unit and Liquid Film Thickness at ( $U_{sl}$ ) = 0.05 - 0.378 m/s	53
4.4 The Correlation of Simulated and Experimental Liquid Hold-up at Varying Viscosity	59
4.5 Performance Evaluation Mean Square Error	61

<b>CHAPTER FIVE</b>	<b>63</b>
<b>5.0 CONCLUSION AND RECOMMENDATIONS</b>	<b>63</b>
5.1 Conclusion	63
5.2 Recommendations	64
5.3 Contributions to Knowledge	64
REFERENCES	66
APPENDIX(CES)	71

## LIST OF FIGURES

<b>Figures</b>	<b>Title</b>	<b>Page</b>
2.1	Horizontal Gas-Liquid flow pattern (Thome and El Hajaj, 2010)	8
2.2	Vertical Gas-Liquid flow pattern (Ren, <i>et al.</i> , 2021)	10
2.3	Slug Flow Diagram (Hernandez-Perez, 2007)	17
3.1	A Schematic Diagram of the Flow Facility (Abdulkadir <i>et al.</i> , 2015)	34
3.2	The Components of the rig (a) Liquid pump (b) Liquid tank (c) Air-Silicone oil (d) Rotameters (e) Cyclone Separator	35
3.3	Overview of the experimental flow facility, (Abdulkadir, 2011)	36
3.4	Random-Forrest Model decision generation based on iterations.	37
3.5	Random Forest algorithm model developed using Python	38
3.6	Flow sheet of the Methodology	39
4.10	Cross plot of simulated and experimental liquid hold up at $U_{sl} = 0.05$ m/s	40
4.11	Cross plot of simulated and experimental Void fraction at $U_{sl} = 0.05$ m/s	40
4.12	Cross plot of simulated and experimental liquid hold up at $U_{sl} = 0.071$ m/s	41
4.13	Cross plot of simulated and experimental void fraction at $U_{sl} = 0.071$ m/s	41
4.14	Cross plot of simulated and experimental liquid hold up at $U_{sl} = 0.095$ m/s	42
4.15	Cross plot of simulated and experimental Void fraction at $U_{sl} = 0.095$ m/s	42
4.16	Cross plot of simulated and experimental Liquid hold up at $U_{sl} = 0.142$ m/s	43
4.17	Cross plot of simulated and experimental Void fraction at $U_{sl} = 0.142$ m/s	43
4.18	Cross plot of simulated and experimental liquid hold up at $U_{sl} = 0.284$ m/s	44
4.19	Cross plot of simulated and experimental void fraction at $U_{sl} = 0.284$ m/s	44
4.20	Cross plot of simulated and experimental Liquid hold up at $U_{sl} = 0.378$ m/s	45
4.21	Cross plot of simulated and experimental void fraction at $U_{sl} = 0.378$ m/s	45
4.22	Cross plot of simulated and experimental Structural Velocity at $U_{sl} = 0.05$ m/s	46

4.23	Cross plot of simulated and experimental Slug frequency at $U_{sl} = 0.05$ m/s	47
4.24	Cross plot of simulated and experimental Slug frequency at $U_{sl} = 0.071$ m/s	47
4.25	Cross plot of simulated and experimental structural velocity at $U_{sl} = 0.071$ m/s	48
4.26	Cross plot of simulated and experimental slug frequency at $U_{sl} = 0.095$ m/s	48
4.27	Cross plot of simulated and experimental Void fraction at $U_{sl} = 0.095$ m/s	49
4.28	Cross plot of simulated and experimental Slug frequency at $U_{sl} = 0.142$ m/s	49
4.29	Cross plot of simulated and experimental Structure velocity at $U_{sl} = 0.142$ m/s	50
4.30	Cross plot of simulated and experimental slug frequency at $U_{sl} = 0.284$ m/s	50
4.31	Cross plot of simulated and experimental Structure velocity at $U_{sl} = 0.284$ m/s	51
4.32	Cross plot of simulated and experimental slug frequency at $U_{sl} = 0.378$ m/s	51
4.33	Cross plot of simulated and experimental Structure velocity at $U_{sl} = 0.378$ m/s	52
4.34	Cross plot of simulated and experimental Length of slug at $U_{sl} = 0.05$ m/s	53
4.35	Cross plot of simulated and experimental Liquid film thickness at $U_{sl} = 0.05$ m/s	53
4.36	Cross plot of simulated and experimental Length of slug at $U_{sl} = 0.071$ m/s	54
4.37	Cross plot of simulated and experimental Liquid film thickness at $U_{sl} = 0.071$ m/s	54
4.38	Cross plot of simulated and experimental Length of slug unit at $U_{sl} = 0.095$ m/s	55
4.39	Cross plot of simulated and experimental Liquid film thickness at $U_{sl} = 0.095$ m/s	55
4.40	Cross plot of simulated and experimental Length of slug unit at $U_{sl} = 0.142$ m/s	56
4.41	Cross plot of simulated and experimental Liquid film thickness at $U_{sl} = 0.142$ m/s	56
4.42	Cross plot of simulated and experimental Length of slug unit at $U_{sl} = 0.284$ m/s	57
4.43	Cross plot of simulated and experimental Liquid film thickness at $U_{sl} = 0.284$ m/s	57
4.44	Cross plot of simulated and experimental Length of slug unit at $U_{sl} = 0.378$ m/s	58
4.45	Cross plot of simulated and experimental Liquid film thickness at $U_{sl} = 0.378$ m/s	58
4.46	Cross plot of simulated and experimental liquid hold up at viscosity = 100 cP	59
4.47	Cross plot of simulated and experimental liquid hold up at viscosity = 5000 cP	60

## CHAPTER ONE

### 1.0

### INTRODUCTION

#### 1.1 Background to the Study

Multiphase flow phenomenon is seen in many engineering fields such as, nuclear reactor engineering, power generation, food production, automobile, and majorly the oil and gas engineering. This phenomenon deals with the concurrent flow of fluids within different phases (i.e., gas, liquid and solid) or the different chemical properties but in the same phase, for example gas-liquid, gas solid, liquid-solid, liquid-liquid and gas-liquid-solid (Abdulkadir *et al.*, 2015).

Where the liquefied gas mixture moves along the pipe, it is observed that different difficulties are encountered in the flow, some of which are phase velocity differences and the existence of numerous flow regimes, flow rate and patterns. The exact nature of flow pattern depends on conduit size and geometry, fluid properties, and phase velocity (Ganat & Hrairi, 2019).

Although pipes are the safest means of transporting oil and gas products, pipelines can sometimes fail, resulting to hazardous consequences and large business losses. The decision to replace, repair, or rehabilitate depends mainly on the condition of the pipeline (El-abbasy *et al.*, 2014). There is therefore a need to asses and predict the condition within the multiphase flow as a key step for pipeline maintenance.

During the co-current flow of gas and liquid in a pipe the multiphase flow can acquire a variety of characteristic distributions called flow regimes, each featuring specific

hydrodynamic characteristics (e.g., bubbly, slug, annular) depending on the volumetric flow rates. (Lakehal, 2013).

Slug flow is an undesirable multiphase flow regime which occurs the most in many industrial processes, causing time varying stresses in pipes and supports and consequently causes structural fatigue damage and failure. The focus of this study is on slug flow regime with air-silicone oil flows in vertical pipes due to its vast usage in oil and gas industry applications. Slug flow pattern has been the dominant flow regime for highly viscous oils occurs over a wide range of superficial velocities, thus making the knowledge of slug flow a major significance for the oil and gas industries.

Experimental, and Numerical approaches in investigating multiphase flow have been significantly done with varying degree of accuracy, however analytical machine learning approach gives an even higher accuracy of prediction. In recent years, the continuing advancement of machine learning makes it a promising data analytic/fusion method for multiphase flowrate estimation (Wang *et al.*, 2020).

In this study, Air-Silicone oil flow data from vertical pipes will be analyzed using machine learning in order to make predictions for slug flow parameters.

## **1.2 Statement of Research Problem**

The challenge associated with slug flow in production facilities including vertical pipe processes has been observed since the 1970s. This undesirable flow pattern continues to demand the attention of researchers and operators alike. Parameters associated with slug flow have been seen difficult to determine accurately and this has a posed a major challenge in flow assurance in industries.

## **1.3 Justification of the Study**

Machine learning in recent years, has been effective in oil and gas operations and predicting multiphase flow because of the possibility of analyzing multiple input parameters and large amount of process data that simple mathematical models are challenged with. Hence, it's use in investigating slug flow regime and making predictions using random-forest-based model as it uses random subspace method and bagging to prevent overfitting in order to improve efficiency and safety in flow assurance in slug flow patterns in vertical pipes.

#### **1.4 Research Aim and Objectives**

The aim of this research is to develop a random forest-based model for predicting liquid hold up and slug flow characteristics in a vertical air-silicone oil 67 mm diameter and 6 m long pipe.

The aim will be achieved through these objectives:

- I. Classification and training time series experimental data in order to develop models for the prediction of Liquid hold up using Machine Learning python interface.
- II. Development of a random forest-based model based derived from the training data
- III. Testing random forest-based model by predicting Liquid hold-up using and other slug flow data using Python interface and a MACRO.
- IV. Validating developed model using relevant performance evaluation metrics.
- V. Testing Random-Forest-based model with high viscosity data viscosity.

## **1.5 Scope of Study**

The studies that will be presented in this work will concentrate on the following:

- I. Characterisation of slug flow regime,
- II. Development of a random forest based model for prediction.
- III. Prediction of liquid hold up and other slug flow characteristics using random forest-based model through machine learning technique
- IV. Validating with relevant performance techniques.

## CHAPTER TWO

### 2.0

### LITERATURE REVIEW

Slug flow is one of the flow assurance challenges confronting the oil and gas industry. This phenomenon can pose significant threat to oil and gas production facilities. The three known types of slug flow: hydrodynamic slug flow, operational induced slug flow, and severe slug flow have been widely investigated (Ehinmowo *et al.*, 2016). Most of the gas-phase is concentrated in large bullet-shaped gas pockets, named Taylor bubbles. The Taylor bubbles are separated by liquid slugs, which contain small entrained gas bubbles. For vertical flow, the liquid film flows downward between the Taylor bubble and the pipe wall. A major characteristic of slug flows is their inherent unsteadiness. It is interesting to note that these two states follow in a random-like manner, inducing pressure, velocity and phase distribution fluctuations. As this kind of flow occurs over a wide range of intermediate flow rates of gas and liquid, it is of significance for many industrial processes employing pipeline transport (Abdulkadir *et al.*, 2014).

The dependence of the flow behavior on different parameters, such as fluid properties, makes it difficult to predict the flow characteristics when one of these parameters is changed. In order to characterize slug flow in more industry relevant fluids, an experimental campaign has been carried out using air and silicone oil as the gas and liquid fluids, respectively. This paper reports the results of an analysis performed on experimental data to determine parameters that characterize the vertical slug flow phenomena observed. A comparison of

the experimental results obtained against previously published empirical relationships is presented.

## **2.2 Flow Regimes Classification in Two Phase Flows**

At the point when at least two phases flow concurrently in pipes, the flow behavior is to a large extent more intricate than for single flow. The phases in general separate because of disparity in density. Shear stresses at the pipe wall are diverse for each phase as a result of their different densities and viscosities. Expansion of the highly compressible gas phase with decreasing pressure increases the in-situ volumetric flow rate of the gas. Consequently, the gas and liquid phases generally do not travel at the same velocity in the pipe. The flow regimes that are present during two or more phase fluid movement depend on the relative magnitude of the forces that act on the fluids.

Buoyancy, turbulence, inertia and surface tension forces vary significantly with flow rates, pipe diameter, inclination angle and fluid properties of the phases.

Two phase flow patterns in vertical tubes are like those in horizontal flows but the distribution of the liquid is dependent on gravity that acts to ensure the liquid is constrained to the bottom of the tube and the gas at the top.

Flow patterns in two phase flow depend on different flow parameters, including the physical properties of fluids (the density of the gas and liquid phases respectively ( $\rho_g$  and  $\rho_l$ ), the viscosity of the gas and liquid phases ( $\mu_g$  and  $\mu_l$ ), and the surface tension ( $\sigma$ )), the flow rate of the gas and liquid phases ( $Q_g$  and  $Q_l$ ), as well as the geometrical dimensions of the flow system.

The flow regimes can be divided into three main classes:

- i. Regimes for horizontal flow in pipes, where the heavier phase (water) tends to be located close to the bottom, because of gravity. In most cases the gas phase pushes the liquid phase along the flow direction.
- ii. Regimes for vertical flow in pipes. The liquid phase tends to be on the pipe walls, forming a stable or an unstable film. Flow velocity can be different and flow regimes form differently for upward and downward flows (Asikolaye, 2019).
- iii. Regimes for sloped pipes, which are not as well known. Here the slope angle is important as well as the direction of the flow (upwards or downwards).

### **2.2.1 Horizontal multiphase flow regimes in pipes**

When gravity is seen to act perpendicularly to the tube axis, separation of the phases can develop. This leads to increases in the possible number of flow patterns, as shown schematic diagram in Figure 2.7.

According to (Monni *et al.*, 2014), the horizontal gas liquid flow can be classified in four general flow structures: bubbly flow, stratified flow, slug/plug flow and annular flow. Each flow pattern can also be divided in sub categories: stratified flow in smooth and wavy flow, intermittent flow in slug and plug flow and annular flow in smooth, wavy and mist flow. The flow patterns according to (Thome and El Hajaj, 2010) are illustrated in Figure 2.1 below.

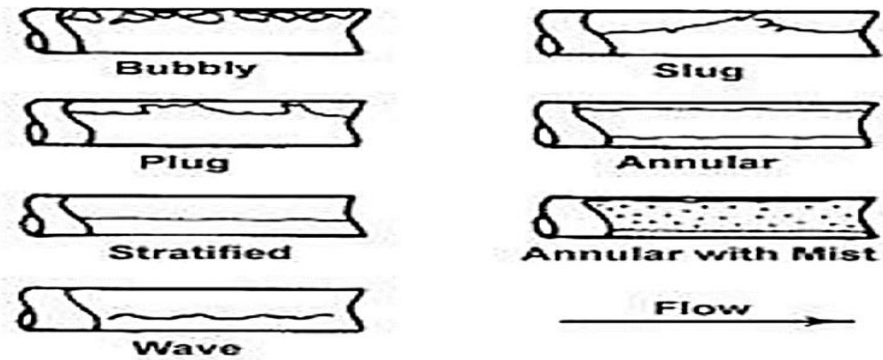


**Figure 2.1:** Horizontal Gas-Liquid flow pattern (Thome and El Hajaj, 2010)

### ***2.2.1.1 Slug flow***

Similar to plug flow, is intermittent. The gas bubbles are larger while smaller bubbles are in the liquid slug. At greater occurring levels of aeration, they are known frothy surges or semi-slug, if the surges do not occupy the pipe completely. However, this might be better considered as part of wavy flow. A continuous gas core with a complete wall film has annular flow characteristics. Just as in vertical flow, some of the liquid can be entrained as drops in the gas core. Gravity causes the film to be thicker on the bottom of the pipe but as the gas velocity is increased the film becomes circumferentially more uniform.

### ***2.2.1.2 Plug flow***

These are liquid plugs separated by elongated gas bubbles. These bubbles are smaller than the tube diameter such that the liquid phase is separated and found below them. This particular flow regime is also known as the elongated bubble flow. Plug flow is characterized by bullet shaped gas bubbles as seen in vertical flow. However here they travel along the top of the pipe (Kwatia, 2016).

### ***2.2.1.3 Bubbly flow***

As in the equivalent pattern in vertical flow, this flow is made up of gas bubbles dispersed in a liquid continuum. However, except at very high liquid velocities when the intensity of the turbulence is strong enough to cause dispersion of the bubbles about the cross section, gravity usually is seen to make bubbles accumulate in the upper part of the pipe as illustrated. In Stratified flow liquid flows in the lower part of the pipe with the gas above it. The interface is smooth. An increase of gas velocity causes waves to form on the interface of stratified flow leading to wave like flows (Kwatia, 2016).

### ***2.2.1.4 Stratified flow***

This particular flow regime occurs at low liquid and gas flow rates, complete separation of the two phases occurs. Since the gas is less dense, it stays at the top and the denser phase being the liquid at the bottom of the tube, such that the horizontal interface between them is undisturbed. This causes a separation between the liquid and the gas in this regime. For gas-liquid flows, the difference in densities of the two fluids is large and the flow ranges over which stratified flow is found, is correspondingly larger.

### ***2.2.1.5 Stratified-wavy flow***

Once the gas flow rate in a stratified flow is increased, the gas velocity tends to increase such that waves are formed on the interface of these fluids. The waves move in the direction of flow with amplitude notable and dependent on the velocity of both phases. As the waves rise up the walls of the pipe, thin films of liquid are left on the wall.

### 2.2.1.6 Annular flow

At higher gas flow rates, the liquid forms a thin film along the walls of the tube, similar to that in vertical flow. However, the liquid film at the bottom is thicker than at the top. The disturbance between the two phases causes droplets to disperse in the core of the gas core.

### 2.2.1.7 Mist flow

As the gas velocities increase in annular flow, the liquid films along the wall are stripped and coalesce into wisps in the gas core.

Various studies have been done in order to understand the behavior of the various flow regimes and to develop models to aid the prediction of these regimes in pipelines.

## 2.2.2 Vertical multiphase flow regimes in pipes

The Figure 2.2 below illustrates the different flow patterns in vertical flow systems in multiphase operations.

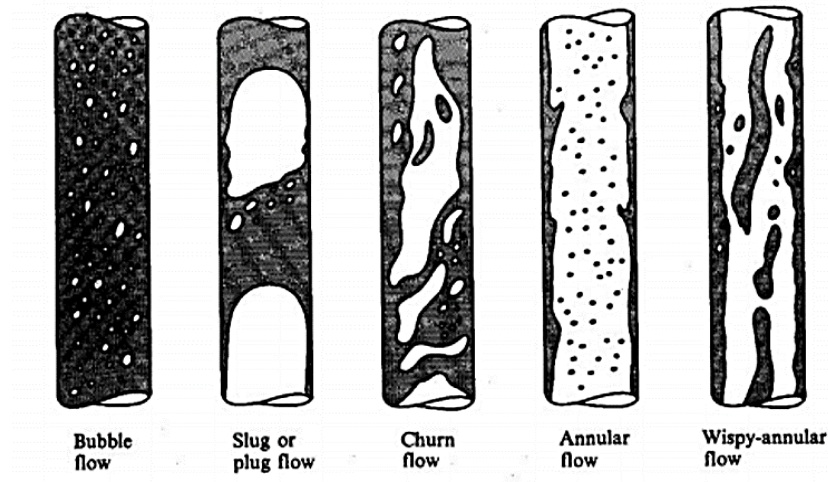


**Figure 2.2:** Vertical Gas-Liquid flow pattern (Ren *et al.*, 2021) (Gas in white, Liquid in grey)

In the oil and gas industry, multiphase flow in vertical pipes often occurs. The flow of fluids through the vertical pipe string causes a loss of energy through friction losses, where the value of this loss depends on the fluid flow viscosity and the size of the conduit. Often, the friction loss is an important part of the oil well completion design (Saeb *et al.*, 2015). The pressure drop occurs as a result of the changes in potential and kinetic energy of the fluid due to the friction on the pipe walls (Shannak, 2008). Generally, the total pressure drop in the vertical conduit is basically related to four main components: frictional, hydrostatic, acceleration, and pressure drop. Among these four components, calculation of the pressure drop is the most complex component and has received extensive attention by researchers. Previous research has tried to determine the two-phase frictional pressure drop in the whole range of flow patterns through a vertical pipe. With experiments carried out to obtain fluid flow friction losses in both Newtonian and non-Newtonian systems (Shannak, 2008; Jiang *et al.*, 2011; Xu *et al.*, 2012; Fadare and Ofidhe, 2009).

A number of experimentations done usually involved the use of short tubes and as a result, a lot of engineering problems are encountered when attempting to extend these experimental set up to realistic process conditions where longer piping is employed. In many experiments, the data shows only a limited number of variables, and as a result, imprecisions are introduced when the friction correlations are applied outside the limitations of the experimental data. As a result of the limited amount of data available for these experiments, the effects of some significant variables were ignored in the early studies (Griffith, 1962).

The precision of the prediction of pressure drop in fluid flow has a significant influence on the fluid flow measurement. In some multiphase conditions, the gas travels at a much

higher velocity than the liquid. Accordingly, the flowing density of the gas–liquid mixture is higher than the corresponding density. Moreover, the liquid’s velocity inside the pipe wall can be different over a short distance and can cause a variable friction loss. The variation in velocity and flow regime of the two phases affect pressure drop computations, meaning that slippage is a consequence of the difference between the combined velocities of the two phases, which is caused by the physical properties of the fluids involved. For single-phase flow, the frictional pressure losses do not normally increase with a decrease in the tubing size or an increase in well production flow rate.

This refers to the existence of a gas phase, which tends to slip by the liquid phase without essentially contributing to its lift. Many researchers have tried to show a relationship between the slippage losses and the friction losses (Tek, 1961). A method for the estimation of gas–liquid flow rates in the vertical pipe has been proposed (Shaban and Tavoularis, 2014). The method was used to calibrate a differential pressure sensor to predict the flow rates of both phases in air–water flow. The estimations were in good agreement with real flow rate measurements. Daev and Kairakbaev (2017) proposed a new model of the liquid flow through pipes that incorporated flow straighteners. The prediction of the flow rate of liquid was studied and the parameters affecting the process of measuring the flow rate of liquid were considered.

An experimental study of the two-phase flow regime and frictional pressure drop inside the pipe was done by Cai *et al.*, (2016). The flow patterns were defined and recorded by a high-speed camera. A new empirical correlation was proposed based on the experimental results to predict the liquid multiplier factor of the test channel. A two-phase flow measurement applying a resistive void fraction meter combined to a venturi, or orifice

plate, was suggested by Oliveira *et al.*, (2009). This method was applied to determine the fluid mass flow rates using an air–water experimental apparatus. The results showed that the flow path has no important effect on the meters in relation to the frictional pressure drop in the experimental process range. The outcomes of the experimental work displayed a mean slip ratio of less than 1.1, when slug and bubbly flow patterns were lower than 70 %.

Several types of spatial distribution of both phases flow patterns may occur depending on the set of fluid properties, flow rates, and on the geometry and inclination of the tube. Realizing the importance of accurately predicting the transition conditions between flow patterns, several authors proposed classifications for upward flow of gas-liquid mixtures in vertical pipes (Barnea, *et al.*, 1980; Hewitt, 1982; Taitel and Dukler, 1976). Five main types of gas–liquid flow patterns are usually identified:

- i. Bubbly Flow or homogeneous
- ii. Annular Flow
- iii. Churn Flow or heterogeneous
- iv. Slug Flow

#### **2.2.2.1 Bubbly flow**

At low void fractions, liquid is seen to be continuous and the gas exists as individual bubbles. Homogeneous flow occurs at low void ages, where the Bubble Size Distribution (BSD) is narrow and there exists little interaction between bubbles, while with increasing voidage on the distribution broadens and bubble coalescence and break-up begin to occur. The boundary between homogeneous and heterogeneous bubbly flow is not well defined, however, bubbly flow to be treated as a single regime. Bubble flow consists of a

continuous liquid phase with the gas phase is dispersed as bubbles within it. The bubbles travel with a complex motion within the flow, may be coalescing and are generally of irregular size.

#### ***2.2.2.2 Churn flow***

This flow regime consists of discontinuous, large irregular plugs of gas flow interspersed with slugs of liquid. Heterogeneous flow occurs at high gas superficial velocities. Due to intense coalescence and break-up, small as well large bubbles appear in this regime, leading to wide bubble size distribution. The large bubbles churn through the liquid, and thus, it is called as churn-turbulent flow. The non-uniform gas hold-up distribution across the radial direction causes bulk liquid circulation in this flow regime (Shaikh and Al-Dahhan, 2007).

#### ***2.2.2.3 Annular flow***

At high enough gas-flow rates only a film of liquid exists at the walls of the tube, with liquid droplets also entrained in the flow. Some authors describe other regimes at higher gas flow rates, including wispy annular flow (Edem and Lao, 2019). Annular flow is characterized by liquid traveling as a film on the channel walls. In fact, for certain flow rates, the majority of the liquid travels as drops, leading to the term mist flow being applied to this flow pattern in some industries.

#### ***2.2.2.4 Slug flow***

Slug flow not only occurs in horizontal pipes but also in pipes with inclination and vertical pipes over vast liquid and gas flow rates. The flow is commonly experienced with operational problems such as operation, enhancement of corrosion-erosion, and structural

problems observed in bends particularly. Slug flow hydrodynamics is complex with unsteady flow behavior characteristics. It has peculiar velocity and pressure distributions. Therefore, the predictions of the liquid hold-up, pressure drop, heat transfer, mass transfer are difficult and challenging. (Abdulkadir *et al.*, 2011)

In up flow in pipes with inclined angles and vertical pipe flow, slug flow is usually the dominant flow pattern, Hernandez-Perez, (2007). This can enhance corrosion, as Kaul (1996) noted that the corrosion rate is accelerated when the flow pattern is slug flow.

The increase of the gas flow rate and, consequently, the concentration of small bubbles, promote coalescence between them, yielding larger bubbles. It is seen that the Taylor bubble was named after Geoffrey Taylor, a British physicist and mathematician notable for his pioneer work on slug flow (Davies and Taylor, 1950), these large gas bubbles are characterized by their bullet shape: a round-shaped nose followed by a cylindrical main body.

The Taylor bubbles are separated by intermediate liquid slugs, which may contain small entrained gas bubbles. A major characteristic of slug flows is their inherent unsteadiness. As this kind of flow occurs over a wide range of intermediate flow rates of gas and liquid, it is of major interest to a wide range of industrial processes that employ pipeline transport systems.

The presence of liquid slugs in the flow system gives an irregular output in terms of gas and liquid flow at the outlet of the system, or at the next processing stage.

This can pose problems to the designer and operator of two-phase flow systems. Pressure drop is substantially higher in slug flow as compared to other flow regimes, and the

maximum possible length of a liquid slug that might be encountered in the flow system needs to be known. (Abdulkadir *et al.*, 2011)

Isolated Taylor bubbles rise almost uniformly in vertical pipes, occupying nearly the entire cross-section of the tube. On its turn, continuous slug flow or bubble train flow is characterized by an almost-periodic rise of Taylor bubbles separated by liquid slugs that may contain small, dispersed bubbles in it. Between a Taylor bubble and the tube wall, the liquid flows downwards as a thin falling film. As it reaches the bottom of the bubble, the annular film enters the liquid slug behind it as an expanding jet, with the possibility of creating a recirculation region known as the bubble wake, depending on the flow conditions. Both the shape of the bubble trailing edge and the wake flow pattern depend on the fluid properties and tube geometry, besides flow conditions. If the separation distance between two Taylor bubbles is small enough, the motion and shape of the trailing bubble get largely affected by the flow in the wake of the leading one: the nose becomes distorted and wavy, its velocity increases, and coalescence between bubbles will occur.

### **2.3 Slug Flow Characteristics**

The phenomenon of slug flow in vertical risers is a usually found under normal operating conditions of a gas- liquid phase flow facility, such as in an oil production riser. A large number of research studies have been carried out in this field over the past three decades. An early contribution to slug flow characterisation research was done by by Nicklin *et al.*, (1962), who proffered an empirical correlation to describe the rise velocity of single Taylor bubble in a static water column. Nicklin's empirical relationship, given by equation (2.1), describes the rise velocity of the Taylor bubble as a linear function of the mixture velocity. For the air-water system considered the value of the constant  $C_0$  was determined to be 1.2.

$$U_N = C_0 U_{LLS} + 0.35 \sqrt{gD} \quad (2.1)$$

### 2.3.1 Rise velocity of Taylor bubble

A cross-correlation was performed on the time varying void fraction data measured by the twin ECT- planes located at 5.0 and 5.089 m above the mixer section at the base of the riser. This allows the determination of the delay time as individual slugs passed between the two planes; and this together with the distance between the planes enabled the calculation of the structure velocity,  $U_N$ . Details of the cross-correlation function used may be found in Hernandez-Perez, (2007).

### 2.3.2 Models for liquid hold-up in vertical pipes

The Figure 2.3 below shows the schematic diagram in gas-liquid slug flow in vertical pipes.

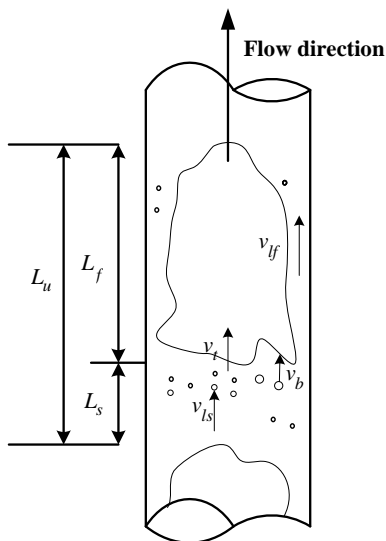


**Figure. 2.3:** Slug Flow Diagram (Hernandez-Perez, 2007).

From the experimental observations, it is seen that slug flow displays alternating liquid and gas flows. In the image of slug flow in a vertical pipe is shown above, the liquid slug that occupies the pipe cross section and it is differentiated by the gas slug, and bubbles may mix in the liquid slug area. There is a liquid film along the wall of the pipe in the gas slug area.

Under the assumptions that liquid film thickness is constant and incompressible liquid and gas phases, the mass balance equation of the whole slug unit liquid can be given as:

$$v_{sl}L_u = v_{ls}H_{ls}L_s + v_{lf}H_{lf}L_f \quad (2.2)$$

Where  $L_u$ ,  $L_s$ , and  $L_f$  are the slug unit length, slug body length, and liquid film region thickness, respectively, m;  $v_{sl}$  is the liquid superficial velocity, m/s;  $v_{ls}$  is the liquid velocity, m/s;  $v_{lf}$  is the velocity of the liquid in the liquid film region, (m/s);

$H_{ls}$  is the liquid hold-up in the slug; and  $H_{lf}$  is the liquid film region liquid hold-up.

Xiao (2011), derived a material balance to the two cross sections. For the liquid phase, the translational velocity balance is given as:

$$(v_t - v_{ls})H_{ls} = (v_t - v_{lf})H_{lf}, \quad (2.3)$$

Where  $v_t$  is the velocity of Taylor bubbles in the liquid film region, m/s.

The total volume flow rate remains constant at any cross section of slug flow as follows:

$$v_M = v_l + v_g = v_{ls}H_{ls} + v_b(1 - H_{ls}), \quad (2.4)$$

Where  $v_M$  is the mixture velocity in the slug, m/s;  $v_b$  is the dispersed bubbles velocity seen in the slug, m/s;  $v_g$  is the superficial gas velocity, (m/s) and  $v_l$  is the superficial liquid velocity, (m/s);

The slug unit liquid hold-up is given as follows:

$$H1 = \frac{H_{ls}.L_s + H_{lf}.L_f}{L_u} \quad (2.5)$$

According to Equations (2.1), (2.2), (2.3), (2.4) and (2.5), the equation provided by Xiao for the liquid hold-up of a slug unit can be expressed as follows:

$$H1 = \frac{v_t.H_{ls} + v_b(1-H_{ls}) - v_{sg}}{v_t} \quad (2.6)$$

Where  $H_{ls}$  is the slug flow liquid hold-up and in Equation (2.6) it can be seen that the solution of the slug flow liquid hold-up of, three parameters are employed: the velocity of Taylor bubbles in the liquid film region  $v_t$ , the velocity of dispersed bubbles in slug  $v_b$ , liquid hold-up of the slug  $H_{ls}$ , and the liquid film region Taylor bubbles  $v_t$ .

Bendiksen (1984) in calculating the Taylor bubbles velocity in the liquid film region at different dip angles proffered the following:

$$v_t = C v_M + 0.35(gD \sin \theta)^{1/2} + 0.54(gD \cos \theta)^{1/2} \quad (2.7)$$

Where  $D$  is the inner diameter of the pipe, m, and  $\theta$  is the angle of inclination, °.

In Equation (2.7),  $C$  is given as the velocity distribution in the slug coefficient. Gokcal *et al.*, (2008) found that when the liquid-phase Reynolds number is low ( $Re_l \leq 1000$ ), the distribution coefficient  $C \approx 2$ . When the distribution coefficient of the liquid phase is higher ( $Re_l > 1000$ ), the distribution coefficient value ranges from Fabre, (2003) is 1.0 – 1.2. Looking at the correlation by Choi *et al.*, (2012). as a relatively simple and accurate equation that takes into account the effect of viscosity as follows:

$$C = \frac{2}{1 + (Re_1/1000)^2} + \frac{1.2 - 0.2\sqrt{\rho_g/\rho_l}(1 - \exp(-18a_G))}{1 + (1000/Re_1)^2} \quad (2.8)$$

$$a_G = 1 - H_1 \quad (2.9)$$

$$Re_1 = \rho_l v_1 D / \mu_l \quad (2.10)$$

Where void fraction is denoted as  $a_G$ ;  $\rho_l$  is the density of the liquid,  $\text{kg/m}^3$ ; and  $\mu_l$  is the viscosity of the liquid,  $\text{Pa s}$ .

The velocity of dispersed bubbles in slug  $v_b$

The dispersed bubbles in slug velocity  $v_b$  is calculated through this equation:

$$v_b = 1.2v_s + 1.35 [\sigma g(\rho_l - \rho_g) / \rho_l]^{1/4} H_{ls}^{0.1} \sin \theta \quad (2.11)$$

Where surface tension is denoted as  $\sigma$ ,  $\text{N/m}$ ; the gas density is given as  $\rho_g$ ,  $\text{kg/m}^3$ ; and

$H_{ls}^{0.1}$  describes “bubble group” effect in the slug.

The liquid hold-up of the slug  $H_{ls}$

In equations (2.8) and (2.10), it is seen that liquid hold-up of the slug not only affects proportionally the liquid hold-up of the slug unit but also considers the influence of slug liquid hold-up on the velocity of dispersed bubbles in the slug. Therefore, slug liquid hold-up is therefore key in determining the liquid hold-up of a slug unit.

Gregory *et al.*, (1978) initially attempted deriving the liquid hold-up of the slug flow through experiments and gave the correlation below between slug liquid hold-up and mixing velocity:

$$H_{ls} = \frac{1}{1 + \left(\frac{vm}{8.66}\right)^{1.39}} \quad (2.12)$$

Gregory *et al.*, (1978) did not however put into consideration the effects the fluid physical parameters and inclination angle brings. According to the experimental results, Felizola, (1992) gave an empirical equation of liquid hold-up of the slug at different angles of inclination (0 – 90°) with velocity of mixing and angle of inclination.

Currently, most studies on slug liquid hold-up are centered on low-viscosity fluid experiments, and the influence of viscosity is not usually discussed. Nadler and Mewes, (1995) researched the effects of liquid-phase viscosity (viscosity: 17, 34 cP) on the liquid hold-up of the slug area, liquid film area, and entire slug unit. In his studies, the flow-averaged liquid hold-up and the liquid hold-up values within the film zone were seen to be greatly higher for oil–air slug flow than the corresponding water–air slug flow values, while the liquid hold-up occurring within the slug zone in oil–air slug flow was lesser than the liquid hold-up in water–air slug flow. As the liquid phase viscosity improved, the average liquid hold-up of the slug unit was seen to be increased greatly. Kora *et al.*, (2011) investigated the oil viscosity effects (181–589 cP) on liquid hold-up slug in a gas–liquid two-phase flow experiment with different viscosities, and the proposed correlation of slug liquid hold-up was compared with correlations proposed by other authors. The results obtained from the research shows that the new model prediction performance was better.

The correlation proposed by Kora *et al.*, (2011) considers the effects of viscosity change on liquid hold-up of the slug. The correlation of slug liquid hold-up is seen below:

$$N_{Fr} = \frac{vm}{(gD^{0.5})}(\rho_l / \rho_l - \rho_g)^{0.5} \quad (2.13)$$

$$N\mu = v_M \cdot \mu_M / gD^2(\rho_l - \rho_g) \quad (2.14)$$

When  $N_{Fr} \cdot Nu^{0.2} \leq 0.15$

$$H_{ls} = 1, \quad (2.15)$$

When  $0.15 < N_{Fr} \cdot Nu^{0.2} < 1.5$ ,

$$H_{ls} = 1.1012e^{(-0.085N_{Fr} \cdot Nu^{0.2})} \quad (2.16)$$

When  $1.5 \leq N_{Fr} \cdot Nu^{0.2}$ ,

$$H_{ls} = 0.9473e^{(0.041N_{Fr} \cdot Nu^{0.2})} \quad (2.17)$$

The slug unit liquid hold-up is calculated thus:

- Estimating  $H_{ls}$  from Equation (2.12), and calculate  $v_b$  according to Equation (2.11). Assuming that  $C = 2$ , calculate  $v_t$  by Equation (2.17) and obtain an initial value  $H_{l0}$  of the average liquid hold-up of the slug by Equation (2.16).
- The initial value  $H_{l0}$  when known,  $v_t$  is calculated by Equation (2.17). The slug liquid hold-up  $H_{ls}$  is obtained from the correlation by Kora, and  $v_b$  could be calculated by from Equation (2.11).
- The liquid hold-up of slug unit  $H_l$  is then calculated using Equation. (2.16); if  $|| H_l - H_{l0} || > 0.001$ , set  $H_{l0} = H_l$ , and repeat step (2). When  $|| H_l - H_{l0} || < 0.001$ , the calculation then terminates.

### 2.3.3 Slug frequency

The slug frequency is defined as the number of units of slugs that traverse in a defined cross-section of a pipe at a given time period. In order obtain the frequency of periodic

structures (slugs), Power Spectral Density (PSD) method was utilized. The Power Spectral Density, PSD, is defined as a measure of how the power in a signal content over frequency and therefore, it describes how the variance of a time series is distributed with frequency. It could be defined mathematically as the Fourier Transform of the autocorrelation sequence of time series. This is determined using a Fast Fourier Transform (FFT) algorithm. Details can be found in Hernandez-Perez, (2007).

### 2.3.4 Length of slug unit, Taylor bubble and liquid slug

The slug unit length is obtained when the rise velocity of the Taylor bubble and the slug frequency is known, as indicated in the equation (2.16). The different zones of the slug unit length have been obtained for varied liquid and gas rates range. The time of passage of the slug unit, Taylor bubble and liquid slug is gotten through analysis of the time series gotten from the twin-planes of the ECT signals. It was assumed that the times to be corresponding to the respective lengths. Relationships were then obtained to estimate the respective lengths, as briefly described below. Equations (2.24), (2.25) and (2.26) is then used to obtain the of the slug unit length, liquid slug as well as the Taylor bubble, respectively.

$$U_N = \frac{L_{su}}{Time} \quad (2.18)$$

$$\text{Where, } \frac{1}{Time} = frequency = f \quad (2.19)$$

$$U_N = L_{SU} * f \quad (2.20)$$

$$L_{SU} = \frac{U_n}{f} \quad (2.21)$$

Assuming that

$L_{SU} \propto t_{SU}$ ,  $L_{TB} \propto t_{TB}$ ,  $L_S \propto t_S$ , incompressibility and Mach number  $< 1$

Dividing  $L_{TB}$  by  $L_S$ ,

$$\frac{L_{tb}}{L_S} = \frac{KT_{tb}}{KT_S} = c \quad (2.22)$$

And also considering the fact that,

$$L_{SU} = L_{TB} + L_S \quad (2.23)$$

The following relationships can be obtained

$$L_{SU} = cL_S + L_S \quad (2.24)$$

$$L_S = \frac{L_{su}}{c+1} \quad (2.25)$$

$$L_{TB} = L_{SU} - L_S \quad (2.26)$$

## 2.4 Parameters to Characterize Flow Regimes

It is important to note when dealing with gas-liquid flow, void fraction and bubble velocity are two of the fundamental parameters. The liquid hold-up and void fraction describes the liquid and gas distribution respectively and is an important parameter for hydrodynamic and thermal design in various multi-phase systems, while the bubble velocity is used to obtain the transport of the void fraction and area concentration of the interface.

### 2.4.1 Void fraction prediction in vertical pipe

Void fraction is the fraction of pipe volume the gas is resident in. This parameter is a major the important parameters used to determine flow pattern characteristics in two-phase flows. It is used for other variables such as two-phase flow viscosity, density, the relative average

velocity of two-phases and for estimation of pattern of flow transitions, heat transfer, interfacial area calculation and determination of pressure drop. It can be measured using wire mesh sensors, quick-close valves,  $\gamma$  rays, x-rays, and microwave, among many others (Oteng, 2014). In considering void fraction, the time average value (taken over a long period) is used, but it should be noted that the void fraction varies as the time varies, hence the need to know the various at different points in time (Almalki and Ahmed, 2019).

#### 2.4.2 Pressure drop prediction in vertical pipes

Prediction of pressure drop in multiphase flow channels is essential for the design of flow equipment. It allows sizing of the pump necessary for the operation of the flow system and enables operators to minimize the occurrence of some multiphase challenges like gas hydrate formation since this impedes on the flow efficiency. The total pressure drop considered in this pipe comprises of three distinct components.

$$\left(\frac{dP}{dz}\right)_{tp} = \left(\frac{dP}{dz}\right)_{fric} + \left(\frac{dP}{dz}\right)_{grav} + \left(\frac{dP}{dz}\right)_{acc} \quad (2.27)$$

Where  $\left(\frac{dP}{dz}\right)_{grav} = \frac{g}{gc} \rho \sin\theta$  is the component due to potential energy or elevation change, it is also referred to as the hydrostatic component.

$\left(\frac{dP}{dz}\right)_{grav} = \frac{f_p V^2}{2gcD}$  is the component due to frictional loss.

$\left(\frac{dP}{dz}\right)_{grav} = \frac{\rho v dv}{gc dL}$  is the component due to kinetic energy change or convective acceleration. According to the definition of flow geometry, when the pipe is in the horizontal position, the angle and the sine of the angle is zero. This means that there is no elevation and hence the pressure drop and pressure gradient becomes;

$$\left(\frac{dP}{dz}\right)_{tp} = \left(\frac{dP}{dz}\right)_{fric} + \left(\frac{dP}{dz}\right)_{acc} \quad (2.28)$$

The pressure drop due to acceleration is often minimal and is mostly overlooked in design calculations

## **2.5 Models in Multiphase Flow**

The need to model and predict the exact behaviour of multiphase flows and the phenomena that they display cannot be over emphasized. There are three broad ways in which such models are usually investigated:

- i. Experimentally, in laboratory, using instruments for measurements,
- ii. Theoretically, through use of appropriate equations of mathematics to model the flow, and
- iii. Computationally, using the power and size of modern computers to address the complexity of the flow.

It is then seen, that there are some applications in which big-scale laboratory models are realistic. But, in reality, the laboratory model varies in terms of scale than the prototype, and then a verified theoretical or computational model is desired for a comfortable extrapolation to the prototype scale. There are certain instances it is difficult to use the laboratory model for a number of reasons. As a result of this, the predictive capability and physical understanding would then depend greatly on theoretical and/or computational models. This then brings to bear the complexity of most multiphase flows presents as a challenge to be resolved. There could be a possibility of the Navier-Stokes equations in computer codes at a future time for each of the phases or components and in order to determine every variable behaviour of a multiphase flow, the fluid movement around and inside every individual particle or drop, the position of every interface. But the processing speed and power of such computer required to do this with 100% accuracy is not realistic at

this point in time due to technological limitations for most of the occurring flows. A normal occurrence is when turbulence is experienced in one or both of the phases, more difficulty is encountered. Therefore, it is necessary to provide simplifications in realistic models of most gas-liquid flows (Brennen, 2005).

## **2.6 Machine Learning for Slug Flow Analysis**

Machine Learning (ML) is that study in computer science that utilizes computation systems in order to provide sense to data similar to human beings (Kristian, 2018).

According to Kristian (2018), ML is a part of artificial intelligence that collects raw data behavior by through an algorithm or method. The main intention of ML is to allow computer systems learn from experience in form data without being explicitly programmed or inputs from human activity.

### **2.6.1 Python**

Python is an object-oriented programming language commonly employed which possess capabilities of a high-level programming language. It is quite portable and easy to learn command makes it very common in usage in recent time. Python was developed by Guido van Rossum in the Netherlands in 1980s to succeed of ‘ABC’ programming language. It has the features of Java and C programming (Nitnaware, 2019).

#### ***2.6.1.1 Why python for data science***

Python is a very common and significant language for Machine learning and data science studies. These common features of Python that makes it attractive and desired for use includes extensive set of packages such as numpy, pandas, scikit-learn, etc., easy

prototyping, collaborative features as well as one unified language irrespective domain used. (Jyothi and Yamaganti, 2019)

### **2.6.2 Artificial neural network (ANN) modelling**

Systems in ANN can be seen as simplified mathematical models of human brain-like systems and they function as parallel distributed computing networks. However, unlike regular computers, which are programmed to carry out specific task, most neural networks must be taught, or trained. They can learn new associations, new functional dependencies and new patterns. Perhaps, a significant advantage of neural networks in performance is their adaptive nature. Neural networks can adjust their weights automatically to optimize their behaviour as to recognize patterns, decision makers, system controllers, predictors, etc. This enables the neural network to perform well even when the environment or the system being controlled changes with time (Abiodun *et al.*, 2018). In Mijwel (2018), it is seen that ANN has a possibility of overfitting data, training takes a long time particularly large data sets among other limitations.

### **2.6.3 Computational fluid dynamics (CFD)**

Computational fluid dynamics (CFD) is one of the most quickly emerging fields in applied sciences. Because it is a numerical tool which relies heavily on experimental or analytical data for validation. CFD mainly deals with the numerical analysis of fluid dynamics problems, which embodies differential calculus. The equations involved in fluid dynamics are Navier–Stokes equations. CFD process consists of three stages: pre-processing, solving, and post-processing. All three processes are interdependent. As much as 90% of effort is used in the meshing (preprocessing) stage. This requires the user to be dexterous and there must be the idea of creating an understandable topology. The next stage is to solve the

governing equations of flow, which is the computer's work. Post-processing has its own delights, and you can impress people by showing flow simulations such as path lines, flow contours, vector plots, flow ribbons, cylinders, and so forth (Jamshed, 2015).

#### **2.6.4 Neuro-fuzzy logic**

The modern techniques of artificial intelligence have found application in almost all the fields of the human knowledge. However, a great emphasis is given to the accurate sciences areas, perhaps the biggest expression of the success of these techniques is in engineering field. These two techniques neural networks and fuzzy logic are many times applied together for solving engineering problems where the classic techniques do not supply an easy and accurate solution. The neuro-fuzzy term was born by the fusing of these two techniques.

Given the wide usage in industrial application, the perception that the development of a fuzzy system with good performance as difficult was common. The challenge of locating membership functions and appropriate rules is frequently a tiring process of attempt and error. Leading to learning algorithms application to the fuzzy systems. The neural networks, that have efficient learning algorithms, had been presented as an alternative to automate or to support the development of tuning fuzzy systems. Gradually, its application spread for all the areas of the knowledge like, data analysis, data classification, imperfections detection and support to decision-making, etc. Neural networks and fuzzy systems can be fused to improve its advantages and to curb the limitation of each one on its own. Neural networks introduce its computational characteristics of learning in the fuzzy systems and receive from them the interpretation and clarity of systems representation. Thus, the disadvantages of the fuzzy systems are compensated by the capacities of the

neural networks. These techniques are complementary, which justifies its use together (Jamshed, 2015).

## **2.7 Challenges in Machine Learning**

While Machine Learning (ML) is rapidly evolving, making significant strides with cybersecurity and autonomous cars, this segment of Artificial Intelligent (AI) as whole still has a long way to go. The reason behind is that Machine Learning has not been able to overcome number of challenges. The challenges that Machine Learning is facing currently are:

- i. **Quality of data:** Having good-quality data for Machine Learning (ML) algorithms is one of the biggest challenges. Use of low-quality data leads to the problems related to data preprocessing and feature extraction.
- ii. **Time-Consuming task:** Another challenge faced by Machine Learning models is the consumption of time especially for data acquisition, feature extraction and retrieval.
- iii. **Lack of specialist persons:** As Machine Learning (ML) technology is still in its infancy stage, availability of expert resources is a tough job.
- iv. **No clear objective for formulating business problems:** Having no clear objective and well-defined goal for business problems is another key challenge for Machine Learning because this technology is not that mature yet.
- v. **Issue of overfitting and underfitting:** If the model is overfitting or underfitting, it cannot be represented well for the problem.
- vi. **Curse of dimensionality:** Another challenge Machine Learning model faces is too many features of data points. This can be a real hindrance.

- vii. Difficulty in deployment: Complexity of the Machine Learning model makes it quite difficult to be deployed in real life.

## **2.8 Application of Machine Learning**

Machine Learning is the most rapidly growing technology and according to researchers we are in the golden year of AI and ML. It is used to solve many real-world complex problems which cannot be solved with traditional approach. Following are some real-world applications of ML:

- i. Sentiment analysis
- ii. Emotion analysis
- iii. Error detection and prevention
- iv. Weather forecasting and prediction
- v. Stock market analysis and forecasting
- vi. Speech synthesis
- vii. Speech recognition

## **2.9 Phase Distribution of an Air-Silicone Flow in a Vertical Pipe**

Manera *et al.*, (2009) compared wire mesh sensors and conductive needle-probes for measurements of vertical two-phase flow parameters using air-water system. They found out that the WMS is a very good candidate for achieving a full mapping of interfacial area density and also for achieving a full three-dimensional reconstruction of gas bubbles. On the other hand, that the needle probe is less intrusive and yields fewer disturbances in the downstream flow.

Shen *et al.*, (2004) studied two-phase distribution in a vertical (0.2 m internal diameter and height 24 m) pipe. They used optical probes and pressure transducers to record local measurements including; void fraction, Sauter mean diameter and pressure loss. From an analysis of their experimental data, they concluded that the phase distribution patterns could be subdivided into basic patterns, namely, wall peak and core peak using the concept of Fisher skewness. However, the weakness of Fisher skewness is its sensitivity to irregular observations at the extremes where the difference between the mean and the value is cubed. Later, Azzopardi *et al.*, (2008) carried out wire mesh sensor studies in a vertical 67 mm internal diameter pipe using air-water as the operating fluids. They measured the radial time averaged void fraction and cross-sectional average time series of void fraction. They determined that the wire mesh sensor was capable of providing insight into the details of phase distributions in a pipe. They expressed the cross-sectional time averaged air void fraction in terms of the gas mass fraction.

Also, these studies were restricted to the use of air-water flow mixtures. Abdulkadir *et al.*, (2010) carried out experimental investigation of phase distributions of two-phase air-silicone oil flow in a vertical pipe using wire mesh sensors (WMS). They found out that reasonably symmetric profiles were obtained when the air-silicone oil was fully developed and that the shape of the profile was strongly dependent on superficial gas velocity. They also found out that symmetric parabolic profiles can be represented as spherical cap bubble and slug flows and that flattened symmetric profile can be represented as churn flow. It was also reported that the cross-sectional void fraction was strongly affected by the superficial gas velocity, whereby the higher the superficial gas velocity, the higher was the observed average void fraction. Also, the steepness parameter decreases with an increase in gas

superficial velocity whilst the c-parameter increases with an increase in gas superficial velocity. The steepness parameter can be used to classify flow regimes; high steepness values represent cap/ bubble flow, intermediate values, slug flow and low values represent churn flow.

They also reported that the radial void fraction increases with gas superficial velocity and that shape of the profile is dependent on the gas superficial velocity. The profiles for cap/ bubble, slug and churn flows are parabolic, semi-flat parabolic, and flat parabolic profiles, respectively based on the radial void fraction distribution.

## **2.10 Application of Vertical Multiphase Flow**

The study of two-phase flows is of great importance for several technological applications. Particularly, gas-liquid two-phase flows are often encountered in a wide range of industrial applications, such as condensers, evaporators, distillation towers, nuclear power plants, boilers, crude oil transportation and chemical plant (Carpintero, 2009).

Micro-scale liquid-liquid flow finds its potential for process intensification in applications like micro reactors, micro mixers, emulsions and materials synthesis (Al-Azzawi *et al.*, 2021).

## CHAPTER THREE

### 3.1 MATERIALS AND METHOD

This chapter discussed the methodology and techniques used; the objectives stated in chapter one. The system consideration that determines the selection of the materials to be used are also discussed.

#### 3.11 Data Acquisition

The Data to be analysed was gotten from experiments carried out by Abdulkadir, (2011). The work is titled “Experimental and Computational Fluid Dynamics (CFD) Studies of Gas-Liquid Flow in Bends” using an inclinable rig ( $-5^{\circ}$  to  $90^{\circ}$ ) in the Chemical Engineering Laboratory of the University of Nottingham. The facility where the experiment was carried out was made up of a testing section made from transparent acrylic glass pipes of 67 mm diameter pipes and 6 m long as shown in Figures 3.2 and 3.3. The fluid mixture used was an air-silicone oil mixture using a state-of-the-art instrument called a Wire Mesh Sensor (WMS). The schematic diagram of the flow facility is shown in Figure 3.1 below.

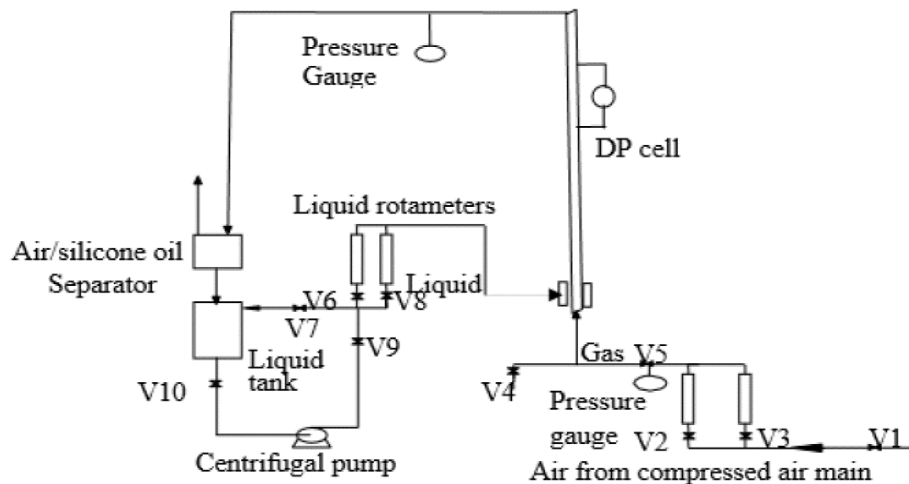


**Figure 3.1:** A Schematic Diagram of the Flow Facility (Abdulkadir *et al.*, 2015)

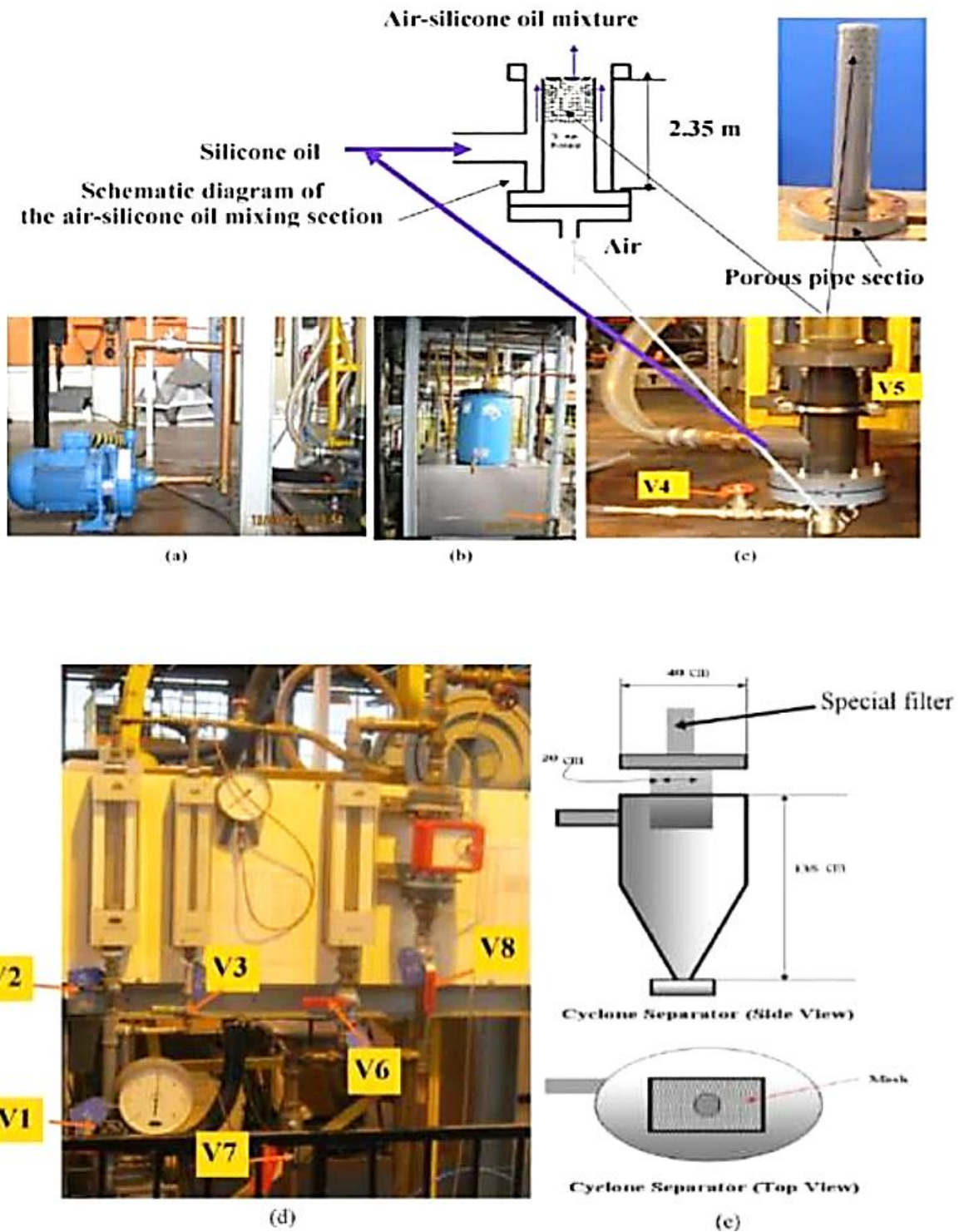


**Figure 3.2:** The components of the rig (a) liquid pump (b) liquid tank (c) air-silicone oil mixing section (d) rotameters and (e) cyclone separator (Abdulkadir, 2011)



**Figure 3.3:** Overview of the experimental flow facility, (Abdulkadir, 2011)

### **3.2 Analysis of Acquired Data**

The wire mesh sensor was used in obtaining the cross-sectional mean liquid hold up time series data. Gas superficial velocity (0.047- 4.727 m/s), at different liquid superficial velocities (0.05-0.378 m/s) on the liquid hold up, were obtained for vertical pipes. The time series raw data was processed to obtain the void fraction for different experimental runs. The void fraction data for planes 1 and 2 of each experimental run were used in a MACRO cross correlation template to obtain the structural velocity after inserting the total number of data (12000), sampling frequency (200 Hz) and distance between the sensors (0.089 m). Power spectral density (PSD) was ran in macro after inserting the total of 12,000 data points and sampling frequency (200 Hz) to obtain the dominant frequency in each run.

#### **3.2.1 Model generation and validation using random forest algorithm**

The Model generation involved using the PYTHON and to learn 70 % of the collected data, 20 % for testing and 10 % for validation.

The model development was based on a random forest algorithm, this choice was influenced due to literature with random forest algorithms efficient in situations and areas where mathematical model fails to handle cumbersome data as well as its convergent nature which uses multiple iterations to get a result as close as possible to the training data as illustrated in g. It was used to predict the liquid hold up for all the various runs of data set.

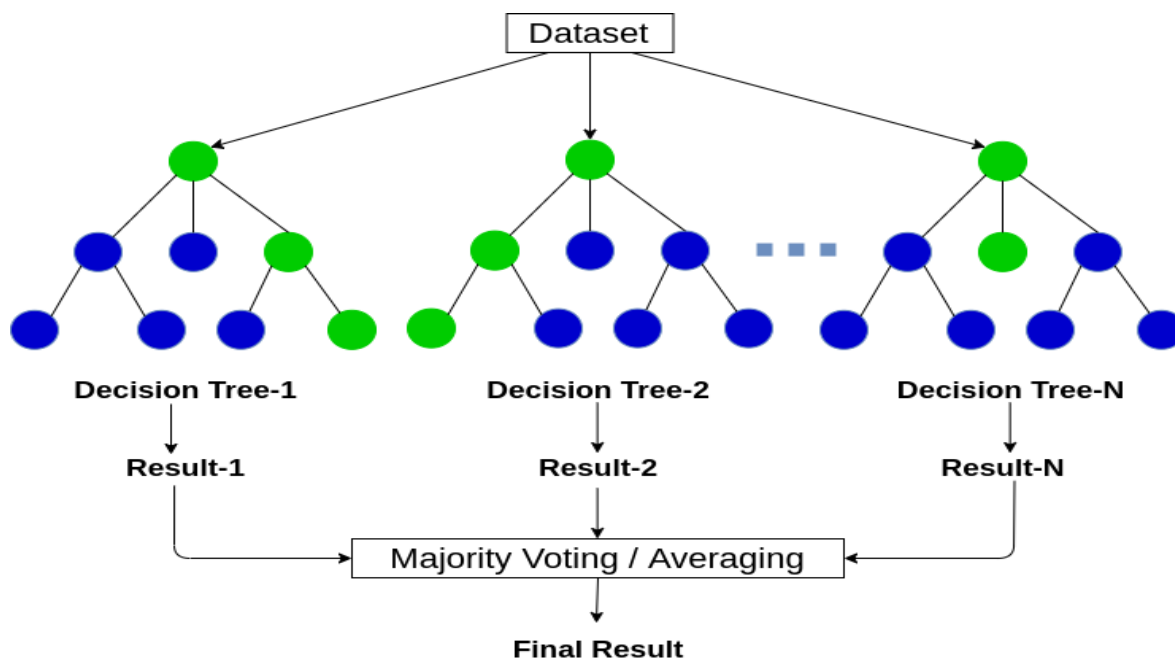


**Figure 3.4:** Random-Forrest Model decision generation based on iterations.

The random-forest based model developed trained with about 70 % of data from Runs 1-13 from the experimental data and tested with about 20 % of data. The algorithm was then used to predict the Liquid Holdup as shown below in Figure 3.5a and b.

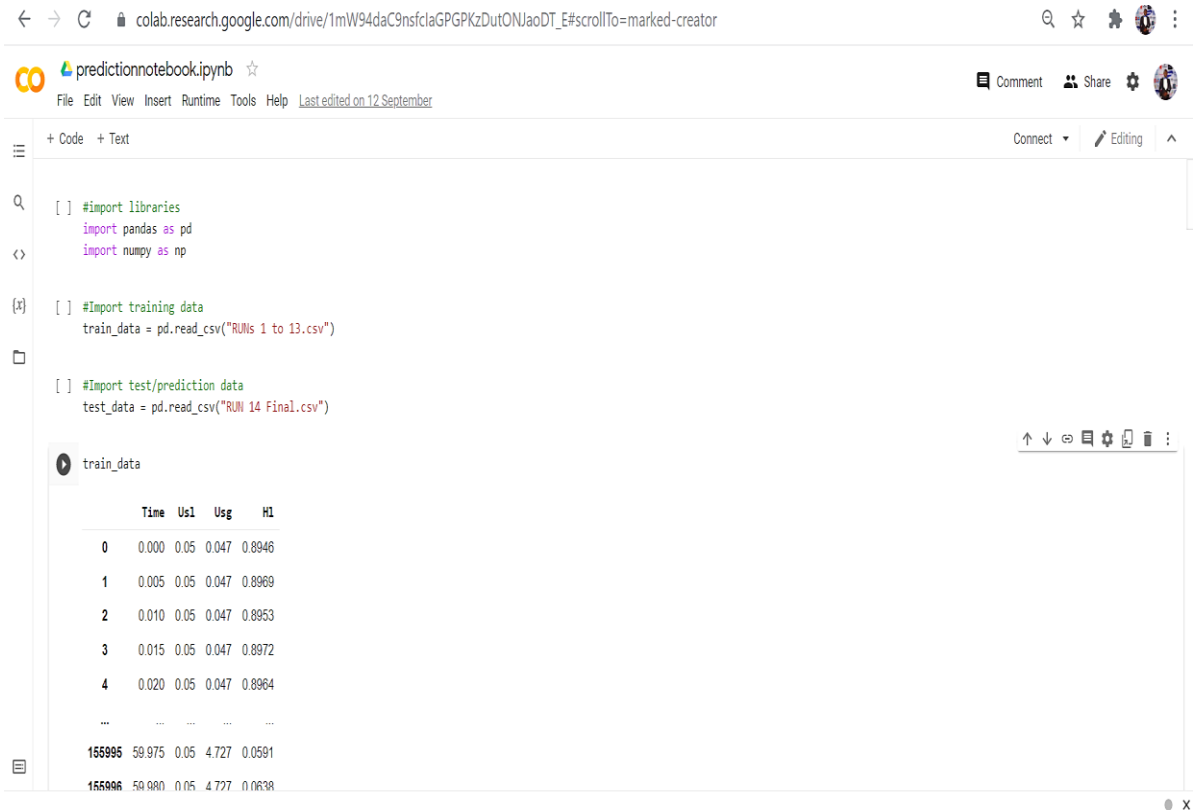


**Figure 3.5a:** Random Forest algorithm model developed using Python

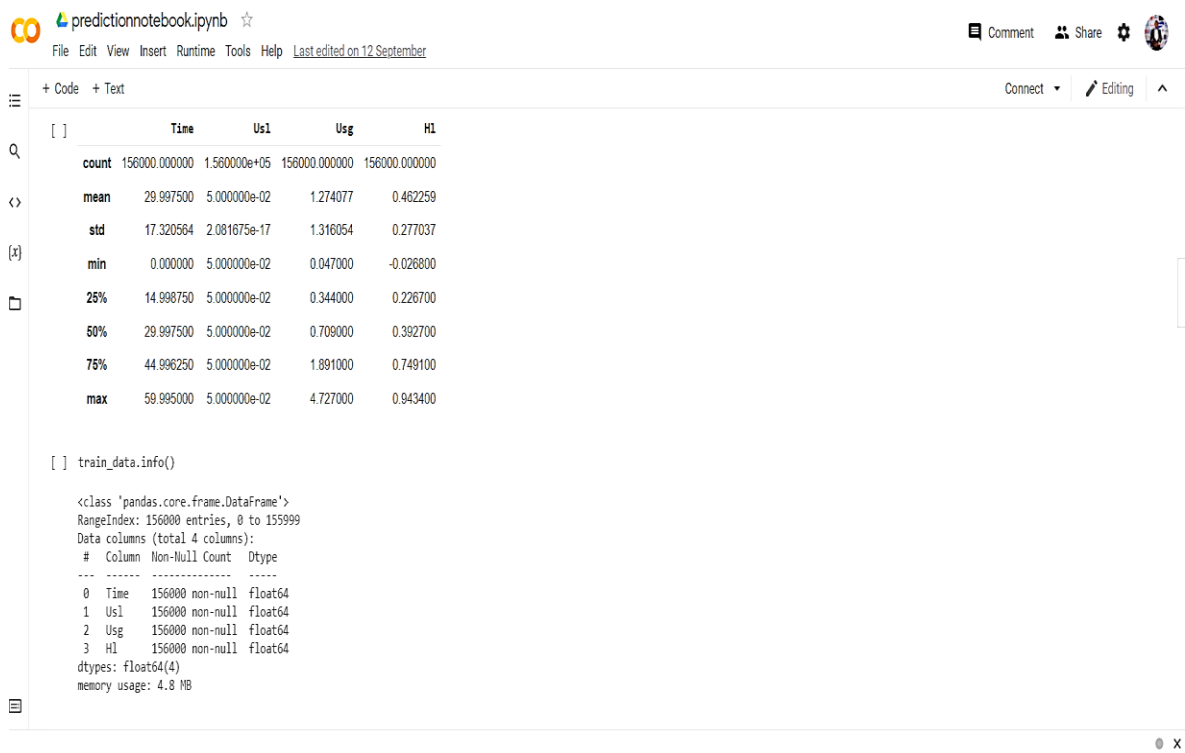


**Figure 3.5b:** Random Forest algorithm model developed using Python

The predicted Liquid Hold up for the various runs data sets were obtained, the Void fraction and slug flow parameters of (Structural velocity, slug frequency, length of slug unit and liquid film thickness) were calculated and then plotted in a cross plot against the experimental to make comparison. The Figure 3.6 below gives the description of the methodology steps taken.

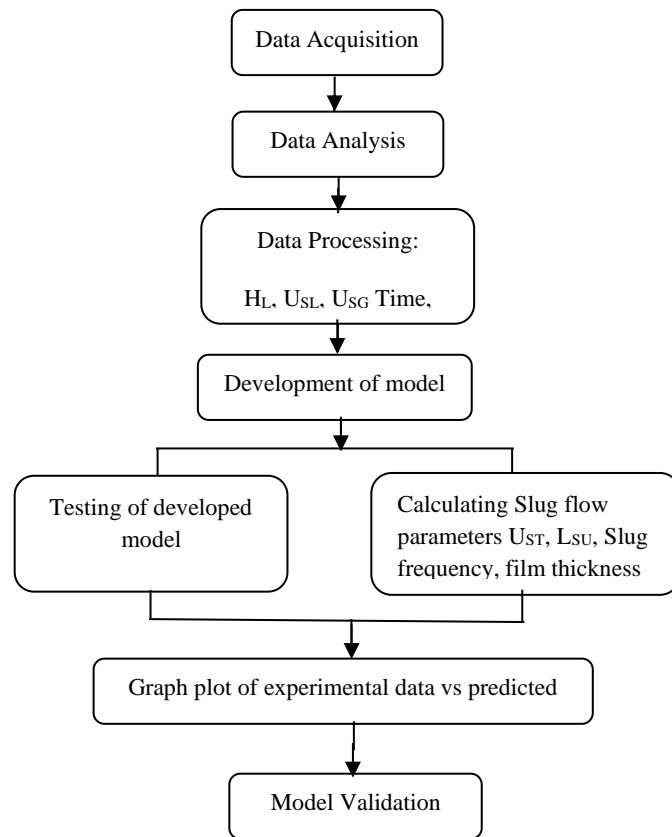


**Figure 3.6:** Flow sheet of the Methodology

## CHAPTER FOUR

### 4.1 RESULTS AND DISCUSSION

#### 4.11 The Correlation of Simulated and Experimental Liquid Holdup ( $H_l$ ) and Void fraction ( $V_f$ ) at Liquid Superficial Velocity ( $U_{sl}$ ) = 0.05 - 0.378 m/s

From the liquid hold up cross plots as shown in Figures 4.10, 4.12, 4.14, 4.16, 4.18, and 4.20, it can be seen that the Liquid hold up decreases with increasing gas velocity at constant liquid velocity, while void fractions in Figures 4.11, 4.13, 4.15, 4.17, 4.19 and 4.21 were increasing as the gas velocity increased as was the case in Abdulkadir, (2010, 2011 and 2015), Kong *et al.*, (2018) and Hernandez-Alvarado *et al.*, (2017). The model could be seen to give a good fit for the predictions of liquid hold up and void fractions.

The Figures 4.10 to 4.21 shows the Liquid Holdup and Void fraction cross plot of the simulated vs experimental liquid hold up and void fraction obtained using the model. A perfect fit can be seen in Figure 4.10 and 4.11 between the experimental and predicted liquid hold up and void fraction at Liquid superficial velocity of 0.05 m/s. This shows the liquid hold up and Void fraction can give a good estimation using the models generated.

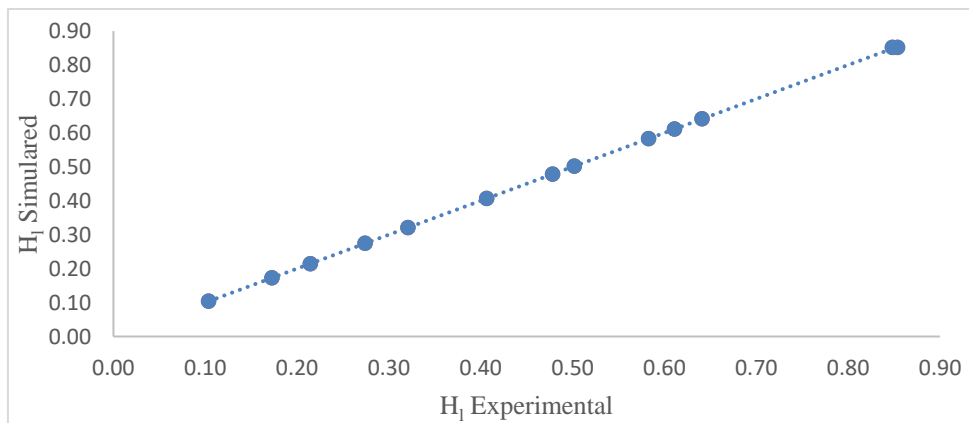


**Figure 4.10:** Cross plot of simulated vs experimental liquid hold up at  $U_{sl} = 0.05$  m/s

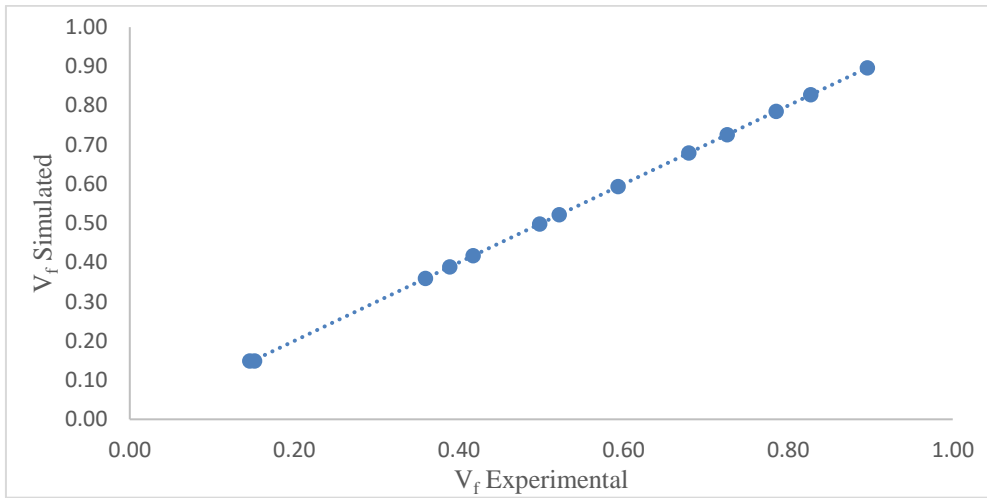


**Figure 4.11:** Cross plot of simulated vs experimental Void fraction at  $U_{sl} = 0.05$  m/s

A near perfect fit between the experimental and predicted liquid hold up and void fraction at Liquid superficial velocity of 0.071 m/s as shown in Figures 4.12 and 4.13 however, with over prediction observed at point (0.54059; 0.498151) for a (x; y) axes respectively for the Void fraction over the range of flow conditions of the present work. Despite this, it can be seen that the liquid hold up and Void fraction can give a good estimation using the models generated.

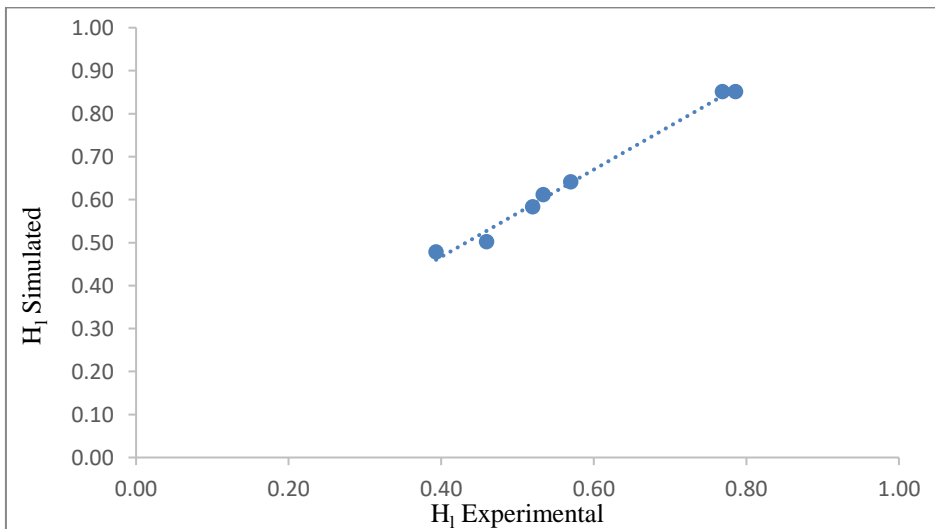


**Figure 4.12:** Cross plot of simulated vs experimental liquid hold up at  $U_{sl} = 0.071$  m/s

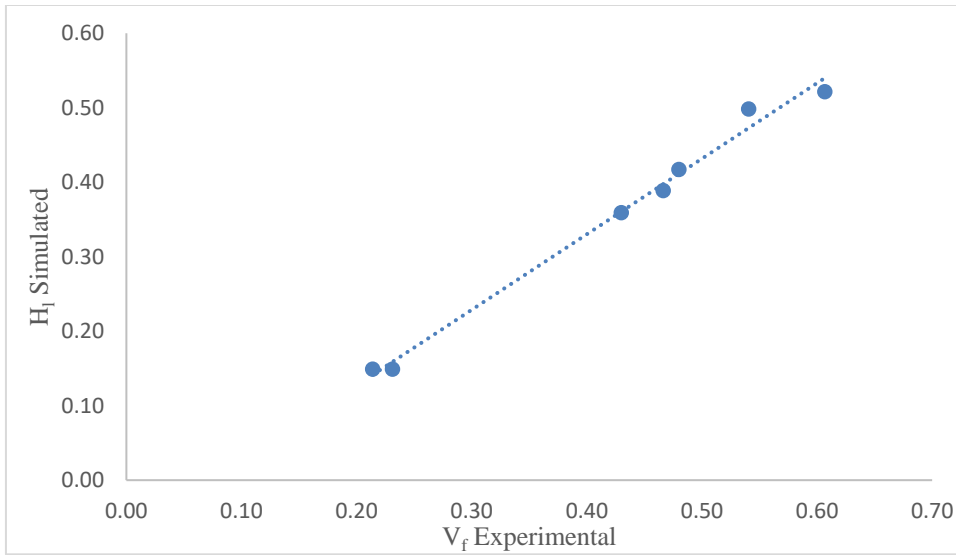


**Figure 4.13:** Cross plot of simulated vs experimental void fraction at  $U_{sl} = 0.071$  m/s

As observed in liquid velocities cross plot, a perfect fit between the experimental and predicted liquid hold up and void fraction at Liquid superficial velocity of 0.142 m/s as shown in Figures 4.14 and 4.15. This shows the liquid hold up and Void fraction can give a good estimation using the models generated for the flow conditions of this work.

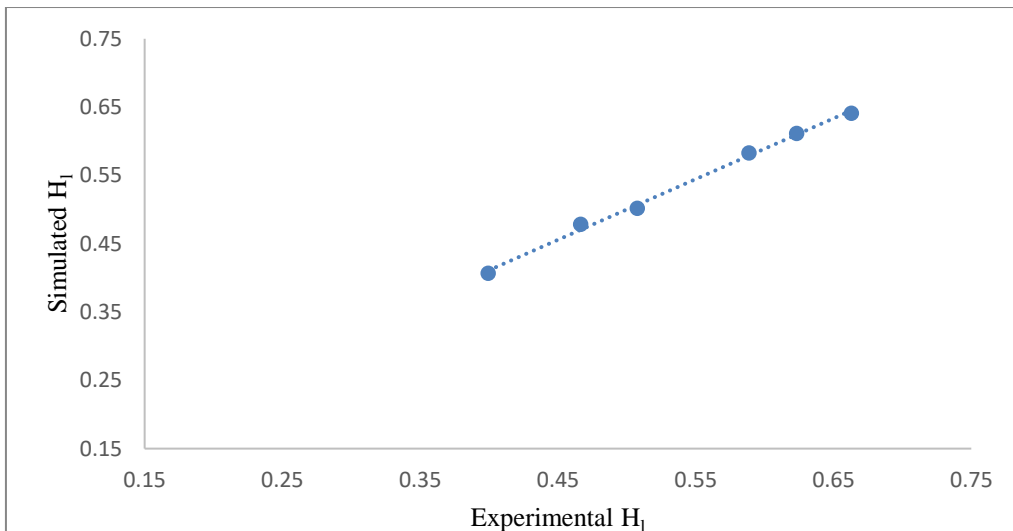


**Figure 4.14:** Cross plot of simulated vs experimental liquid hold up at  $U_{sl} = 0.095$  m/s

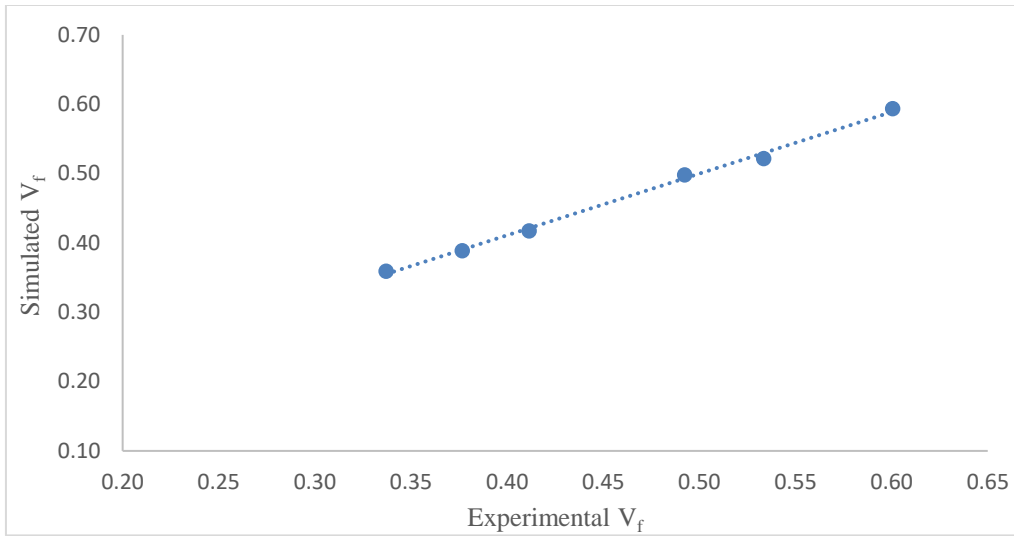


**Figure 4.15:** Cross plot of simulated vs experimental Void fraction at  $U_{sl} = 0.095$  m/s

A perfect fit between the experimental and predicted liquid hold up and void fraction at Liquid superficial velocity of 0.05 m/s in Figures 4.16 and 4.17. This shows the liquid hold up and Void fraction can give a good estimation using the models.

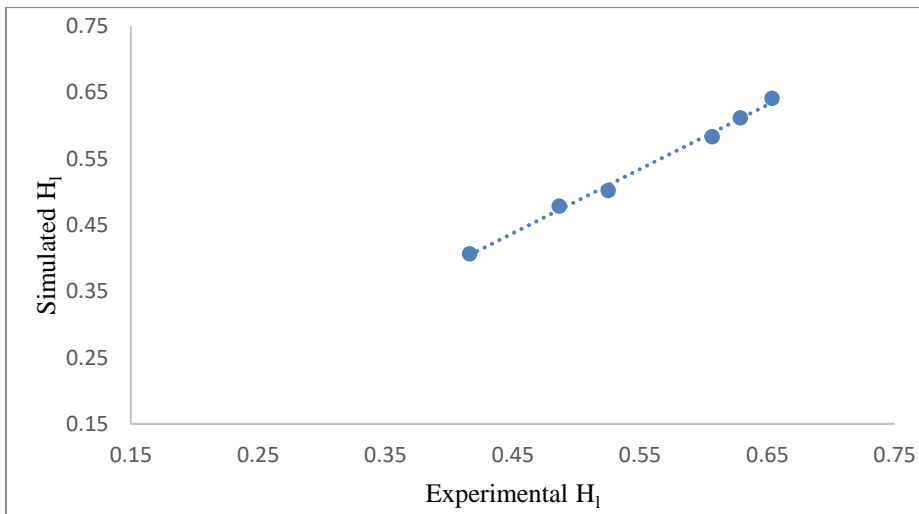


**Figure 4.16:** Cross plot of simulated vs experimental Liquid Hold up at  $U_{sl} = 0.142$  m/s

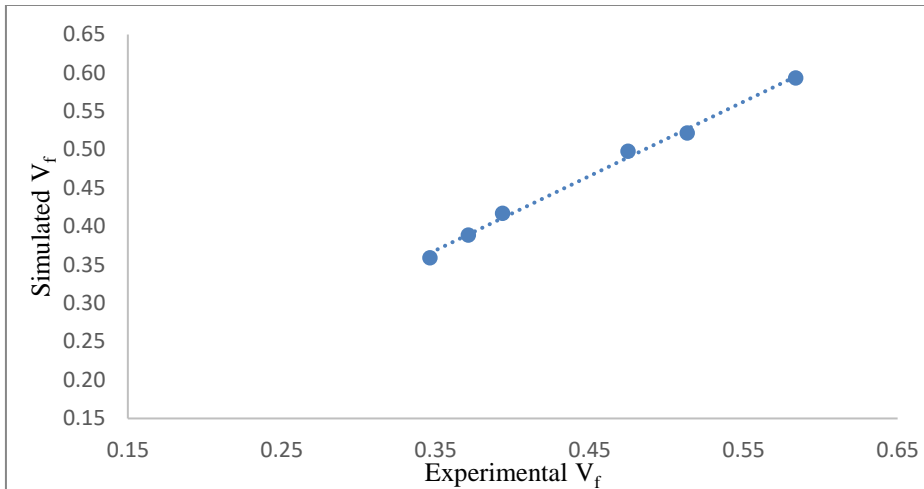


**Figure 4.17:** Cross plot of simulated vs experimental Void fraction at  $U_{sl} = 0.142$  m/s

It can be observed that a perfect fit between the experimental and predicted liquid hold up and void fraction at Liquid superficial velocity of 0.284 m/s as shown in Figures 4.18 and 4.19, However, there were slight over predictions and under predictions observed as the liquid increased to 0.284 m/s. This shows the liquid hold up and Void fraction can give a good estimation using the models.

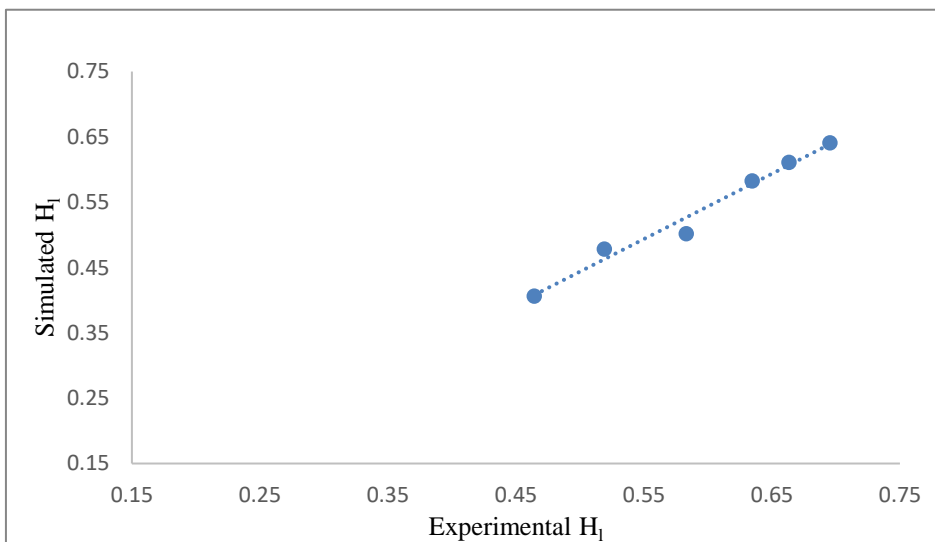


**Figure 4.18:** Cross plot of simulated vs experimental liquid hold up at  $U_{sl} = 0.284$  m/s

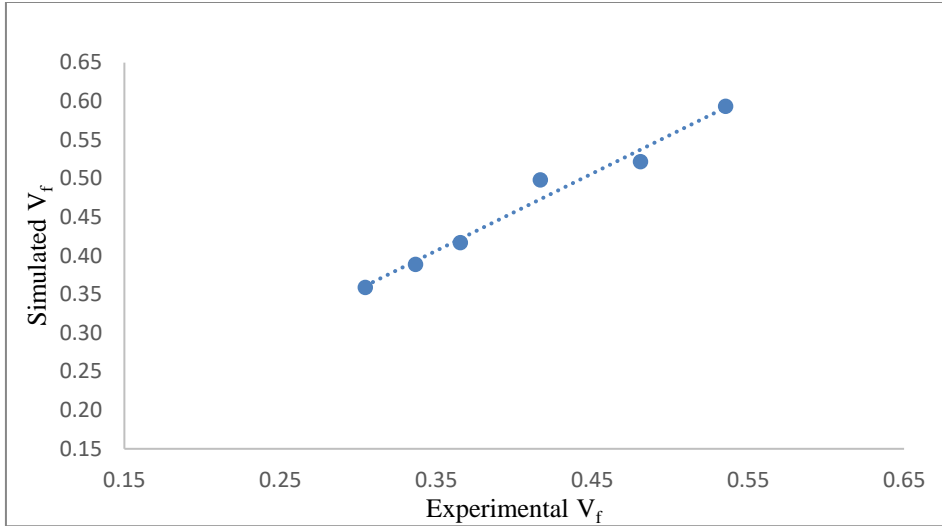


**Figure 4.19:** Cross plot of simulated vs experimental void fraction at  $U_{sl} = 0.284$  m/s

It is shown that a perfect fit between the experimental and predicted liquid hold up and void fraction at Liquid superficial velocity of 0.378 m/s in Figures 4.20 and 4.21 however, there were slight over predictions and under predictions observed as the liquid increased to 0.378 m/s. This shows the liquid hold up and Void fraction can give a good estimation using the models.

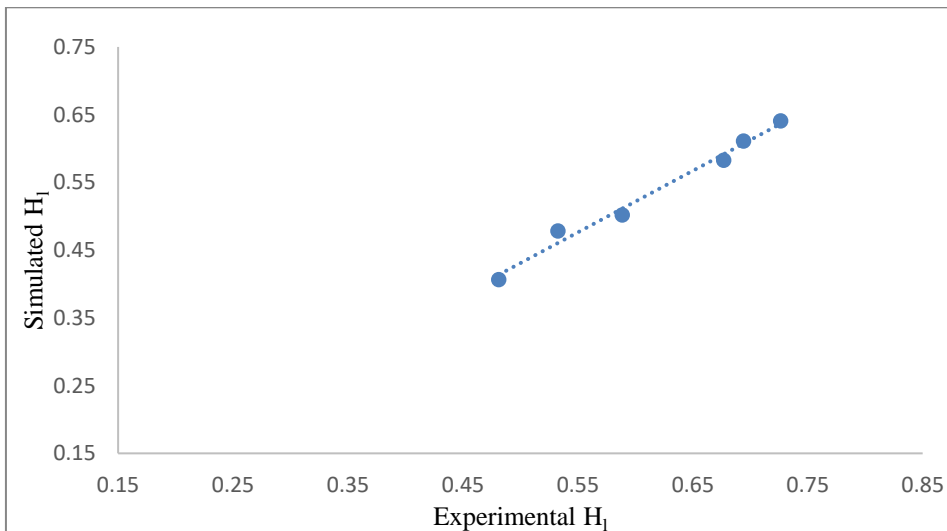


**Figure 4.20:** Cross plot of simulated vs experimental Liquid hold up at  $U_{sl} = 0.378$  m/s

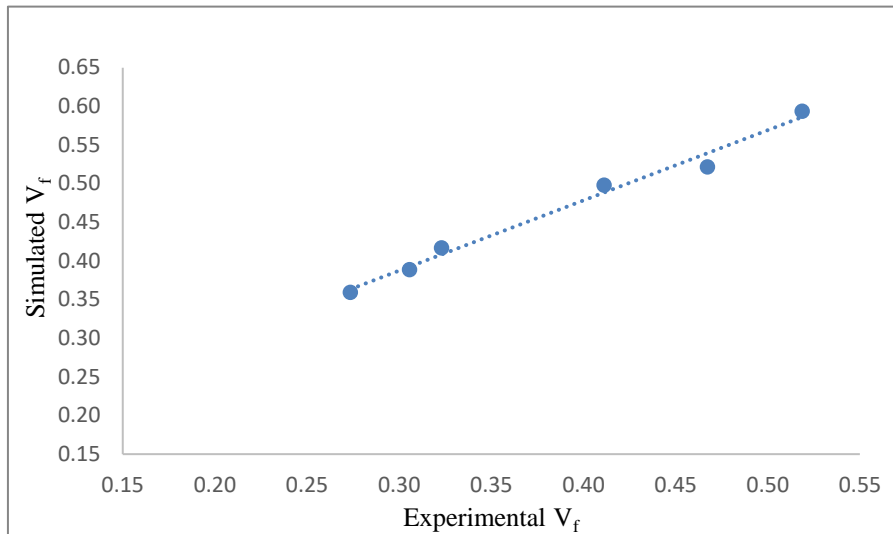


**Figure 4.21:** Cross plot of simulated vs experimental void fraction at  $U_{sl} = 0.378$  m/s

#### **4.2 The Correlation of Simulated and Experimental of Structural Velocity and Slug Frequency at ( $U_{sl}$ ) = 0.05 - 0.378 m/s**

The model failed to predict accurately the structure velocity and this is due to data leakage where the parameters of gas velocity time series is not sufficient in determining structure velocity considering the flow conditions of the work. In Figures 4.22 - 4.33 below are the structure velocity and cross plots of between liquid velocities ( $U_{sl}$ ) of 0.05 to 0.378 m/s.

However, a perfect fit between the experimental and predicted Structural velocity at Liquid superficial velocity of 0.05 m/s in Figure 4.22 under the flow conditions of this work, while as shown in Figure 4.23 the model did not give a good estimate of the predicted slug frequency.

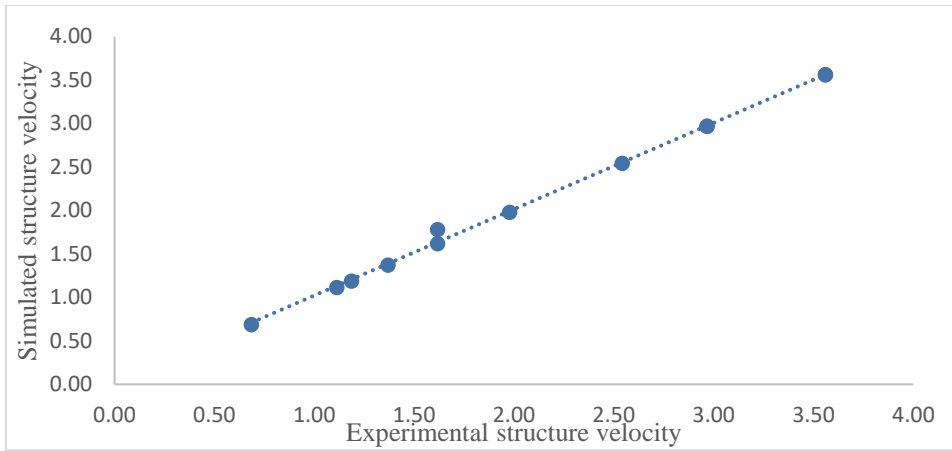


**Figure 4.22:** Cross plot of simulated vs experimental Structural Velocity at  $U_{sl} = 0.05$  m/s

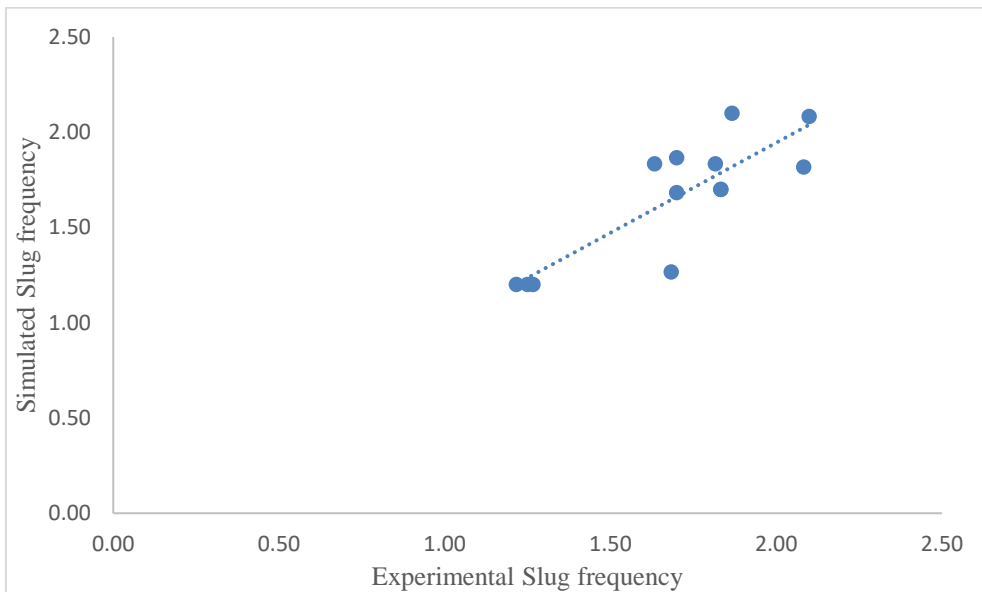


**Figure 4.23:** Cross plot of simulated vs experimental Slug frequency at  $U_{sl} = 0.05$  m/s

Over prediction is observed by the model at liquid velocity of 0.071 m/s for slug frequency as shown in Figure 4.24, while in Figure 4.25 cross plot of structural velocity gives a negative trend this could be attributed to oscillation that could be because from flow transitions.

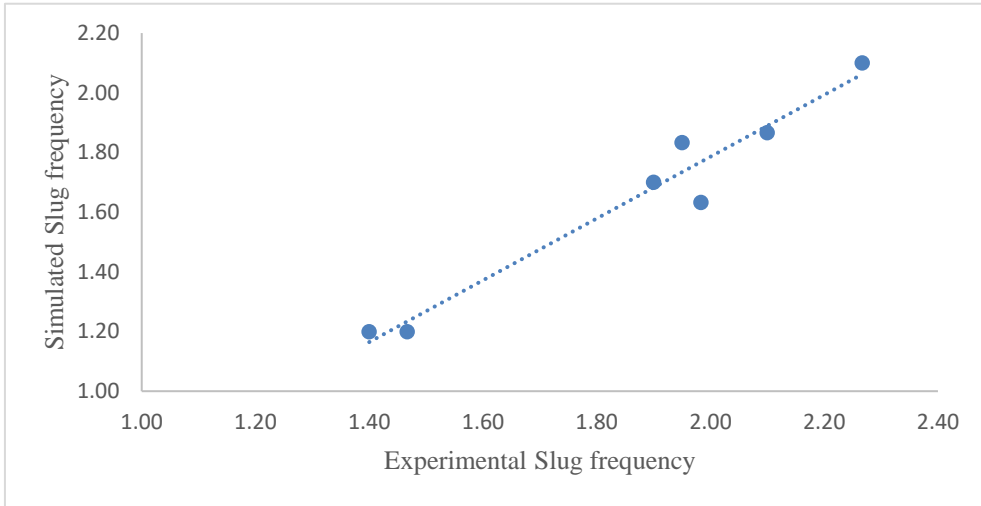


**Figure 4.24:** Cross plot of simulated vs experimental Slug frequency at  $U_{sl} = 0.071$  m/s

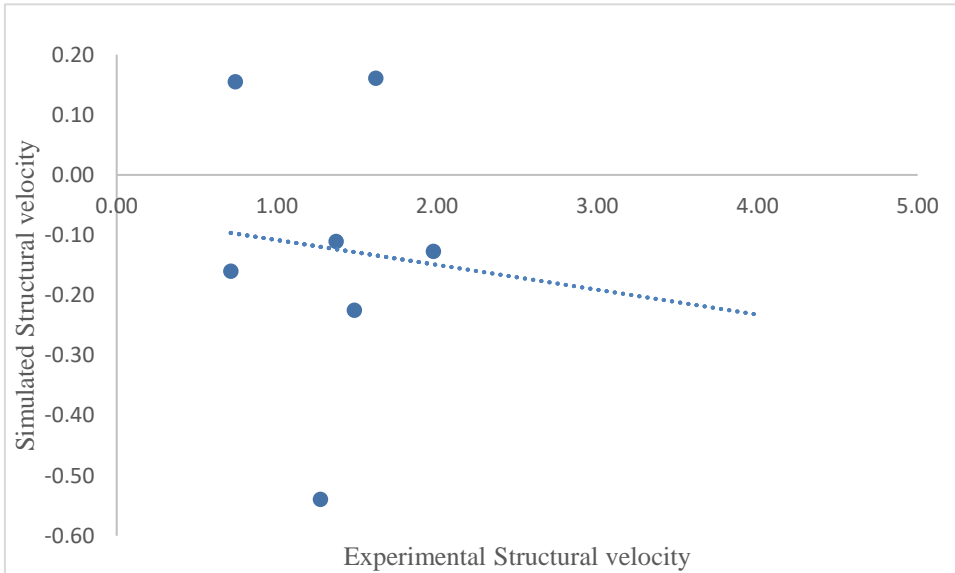


**Figure 4.25:** Cross plot of simulated vs experimental structural velocity at  $U_{sl} = 0.071$  m/s

Wide over prediction is observed by the model as the liquid velocity increased to 0.095 m/s for slug frequency as shown in Figure 4.26, while in Figure 4.27 cross plot of structural velocity gives a negative trend this could also be attributed to oscillation that could come from flow transitions.

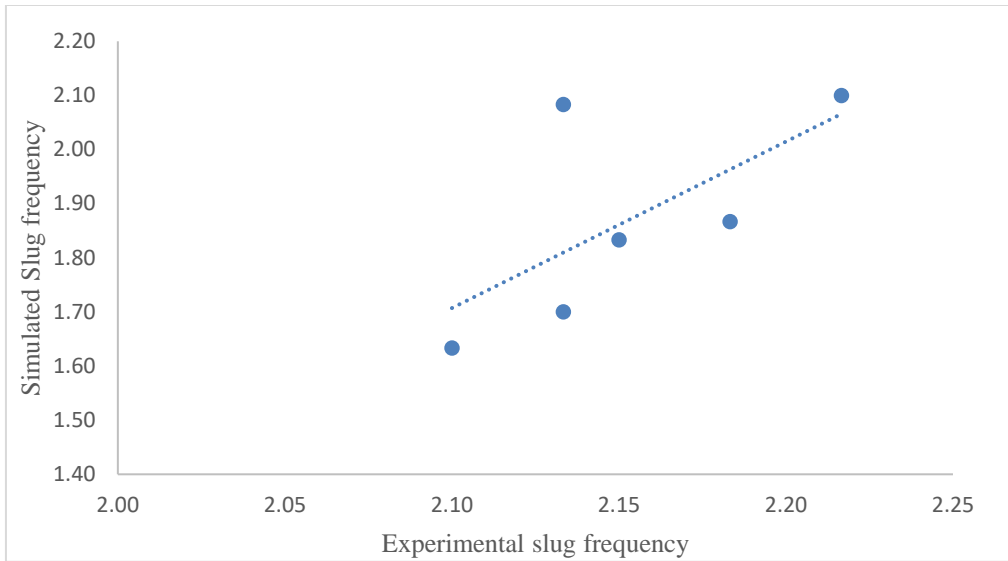


**Figure 4.26:** Cross plot of simulated vs experimental slug frequency at  $U_{sl} = 0.095$  m/s

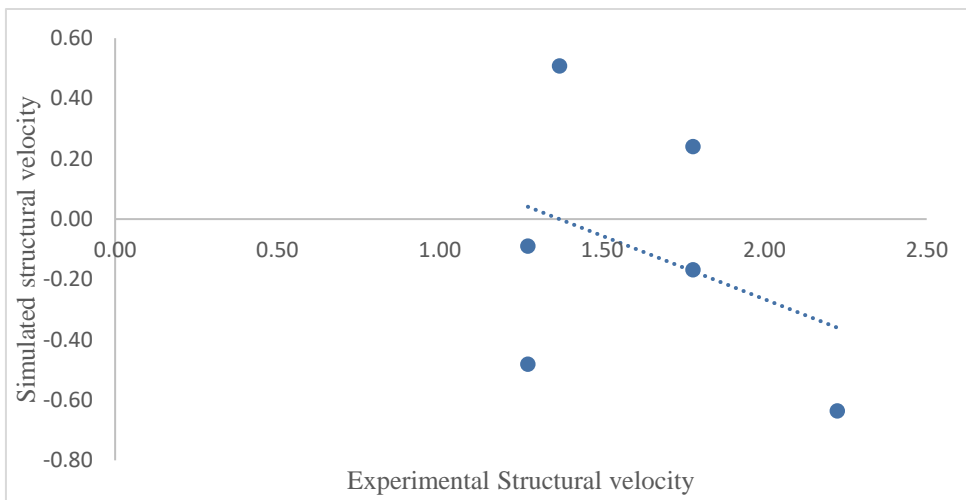


**Figure 4.27:** Cross plot of simulated vs experimental Void fraction at  $U_{sl} = 0.095$  m/s

Similarly, over prediction is observed by the model as the liquid velocity increased to 0.095 m/s for slug frequency as shown in Figure 4.28, while in Figure 4.29 cross plot of structural velocity gives a negative trend this could also be attributed to oscillation that could come from flow transitions.

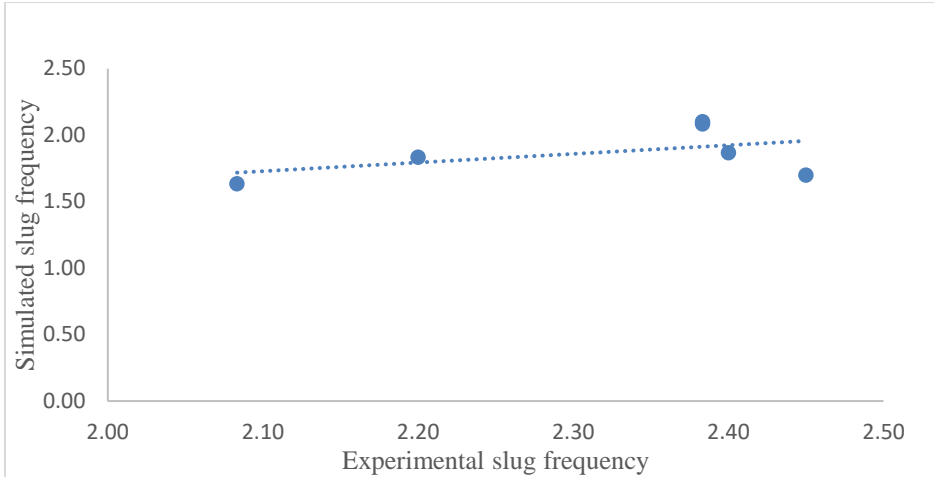


**Figure 4.28:** Cross plot of simulated vs experimental Slug frequency at  $U_{sl} = 0.142$  m/s

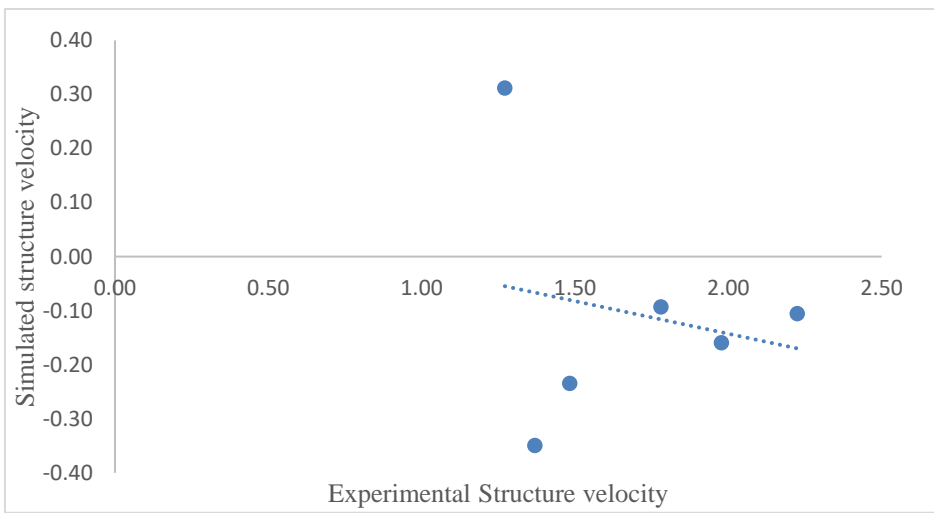


**Figure 4.29:** Cross plot of simulated vs experimental Structure velocity at  $U_{sl} = 0.142$  m/s

Slight over prediction at (2.7333; 2.1000) is observed by the model as the liquid velocity increased to 0.284 m/s for slug frequency as shown in Figure 4.30, while in Figure 4.31 cross plot of structural velocity gives a negative trend, this could also be attributed to oscillation that could come from flow transitions.

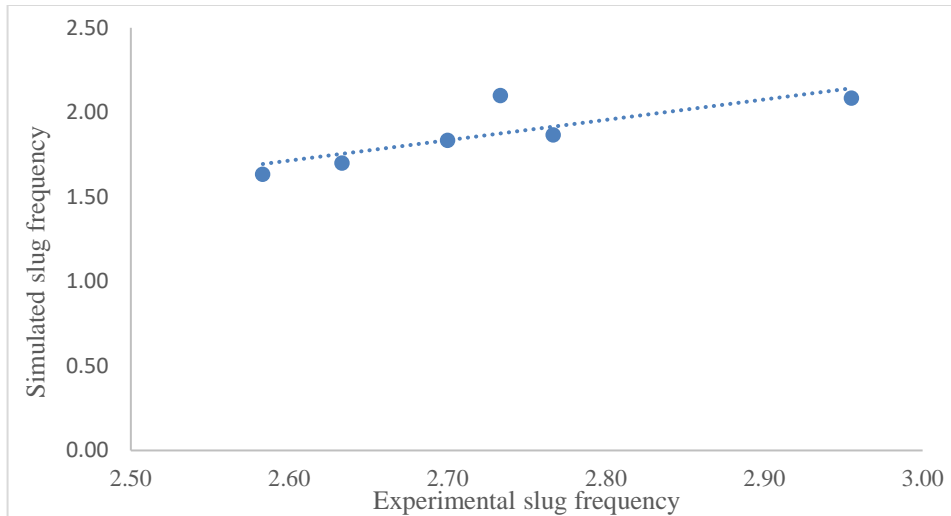


**Figure 4.30:** Cross plot of simulated vs experimental slug frequency at  $U_{sl} = 0.284$  m/s

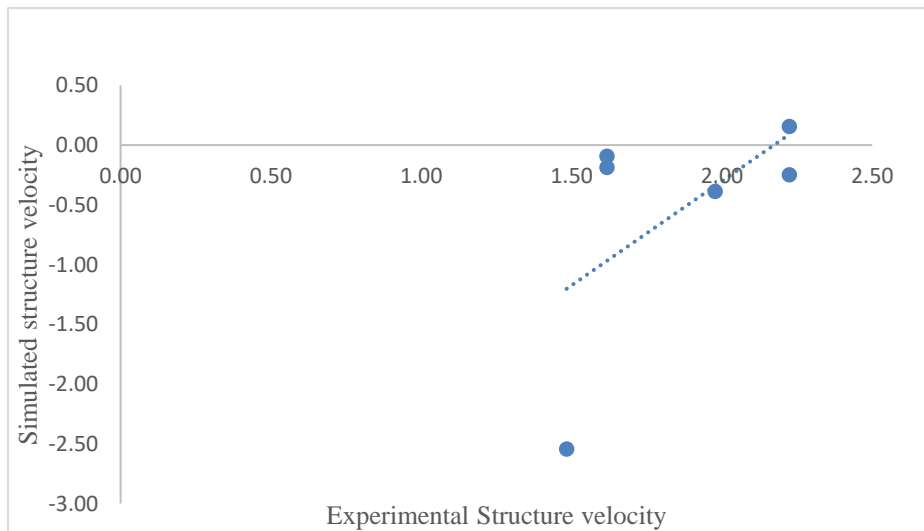


**Figure 4.31:** Cross plot of simulated vs experimental Structure velocity at  $U_{sl} = 0.284$  m/s

As the liquid velocity increased to 0.378 m/s, the cross plot of slug frequency shows the model over and under predicts the slug frequency as well as a negative plot due to increased liquid velocity in the pipe flow as seen in Figure 4.32. Also, in Figure 4.33, there were also over predictions and oscillations observed in the structure velocity.

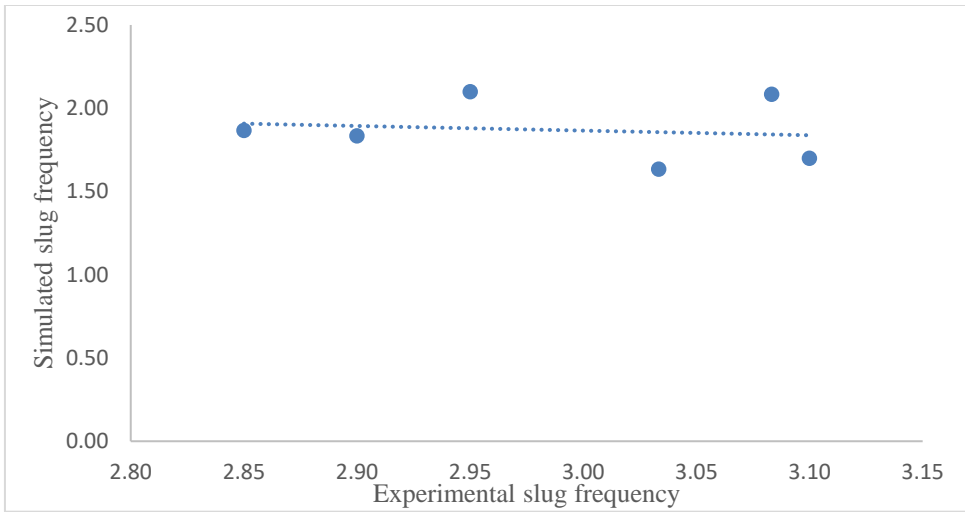


**Figure 4.32:** Cross plot of simulated vs experimental slug frequency at  $U_{sl} = 0.378$  m/s

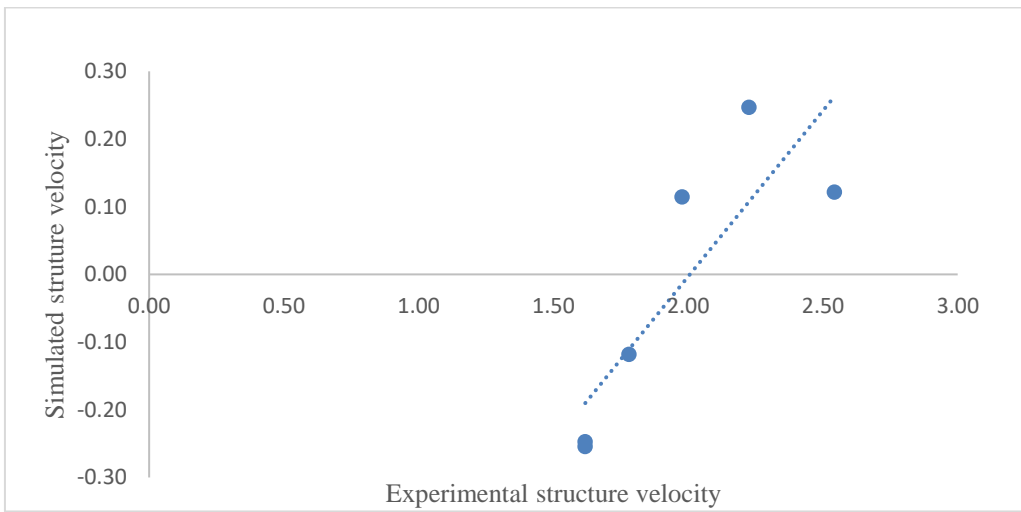


**Figure 4.33:** Cross plot of simulated vs experimental Structure velocity at  $U_{sl} = 0.378$  m/s

### 4.3 The Correlation of Simulated and Experimental Length of Slug Unit and Liquid Film Thickness at Liquid Velocity ( $U_{sl}$ ) = 0.05 - 0.378 m/s

The Figures below 4.34 – 4.3 are the cross plots for simulated vs experimental slug length from 0.05 to 0.378 m/s. The deviations indicated the machine learning model is very limited due to great deviations in the cross plot for predicting length of slug unit since limitations are also seen in the calculation of structure velocity.

There were observed over predictions the length of slug unit this is due to the fact that it is a function of mixture velocity and slug frequency as shown in Figures 4.34. While a perfect fit between the experimental and predicted liquid film thickness at Liquid superficial velocity of 0.05 m/s was observed in Figure 4.35, this shows a good estimate of the liquid film thickness can give a good estimation using the models for liquid superficial velocities as low as 0.05 m/s.

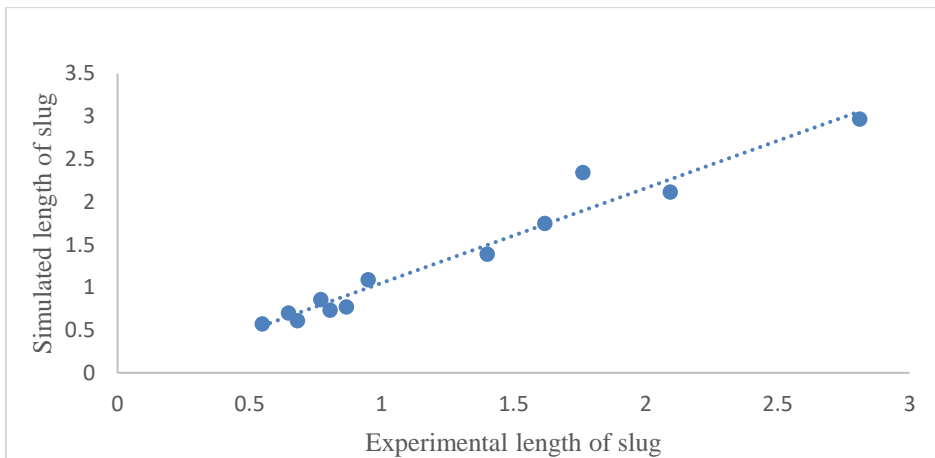


**Figure 4.34:** Cross plot of simulated vs experimental Length of slug at  $U_{sl} = 0.05$  m/s

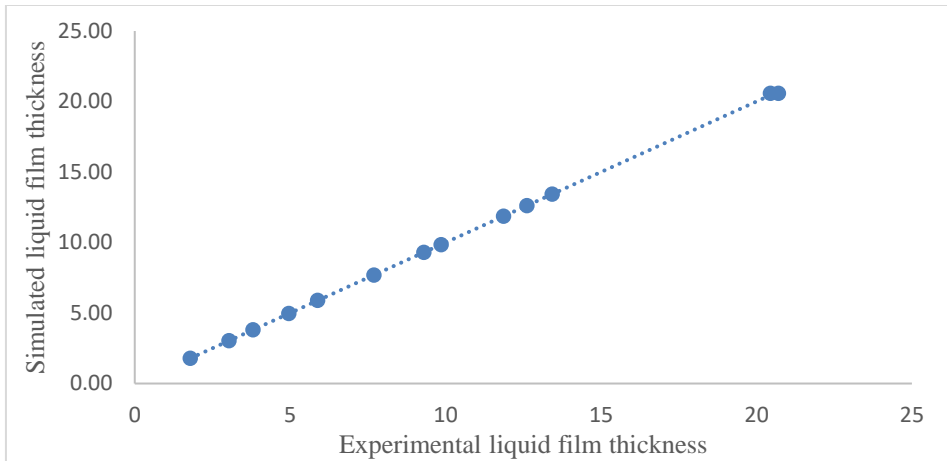


**Figure 4.35:** Cross plot of simulated vs experimental Liquid film thickness at  $U_{sl} = 0.05$  m/s

There was little correlation between experimental and simulated the length of slug unit this is due to the fact that it is a function of mixture velocity and slug frequency, which has limitations in Figure 4.36. While a good fit between the experimental and slight over predictions of liquid film thickness at Liquid superficial velocity of 0.05 m/s was observed as seen in in Figure 4.37, this shows good estimation can be gotten using the model for liquid superficial velocities as low as 0.071 m/s.

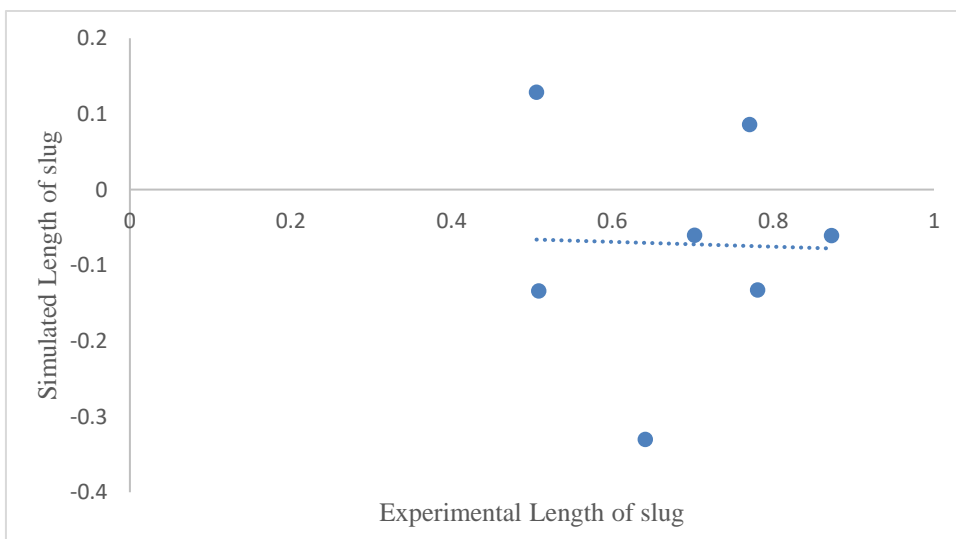


**Figure 4.36:** Cross plot of simulated vs experimental Length of slug at  $U_{sl} = 0.071$  m/s

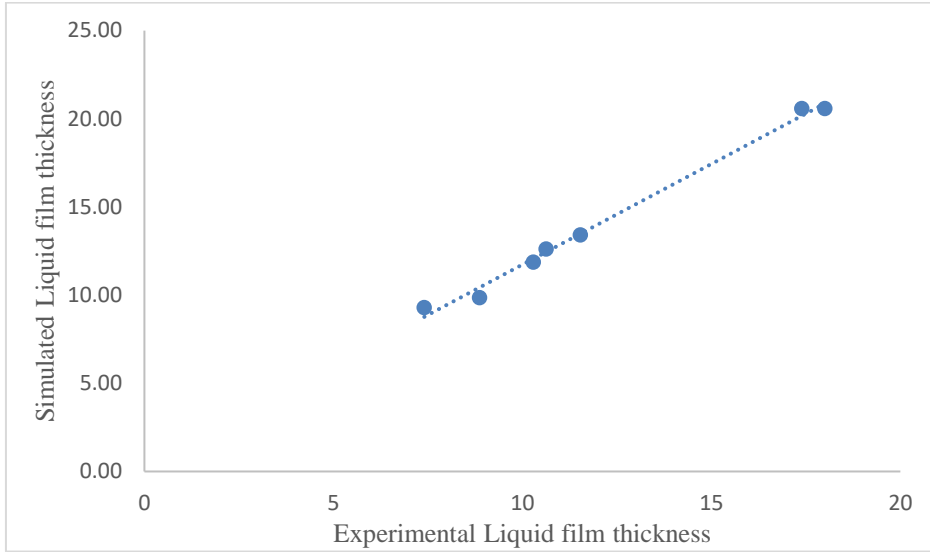


**Figure 4.37:** Cross plot of simulated vs experimental Liquid film thickness at  $U_{sl} = 0.071$  m/s

There was little correlation between experimental and simulated the length of slug unit this is due to the fact that it is dependent on mixture velocity and slug frequency, whose prediction has limitations from the random forrest model as shown in Figure 4.38. While in a good fit between the experimental and slight over predictions of liquid film thickness at Liquid superficial velocity of 0.095 m/s was observed in Figure 4.39, this shows very good estimation can be gotten using the model.

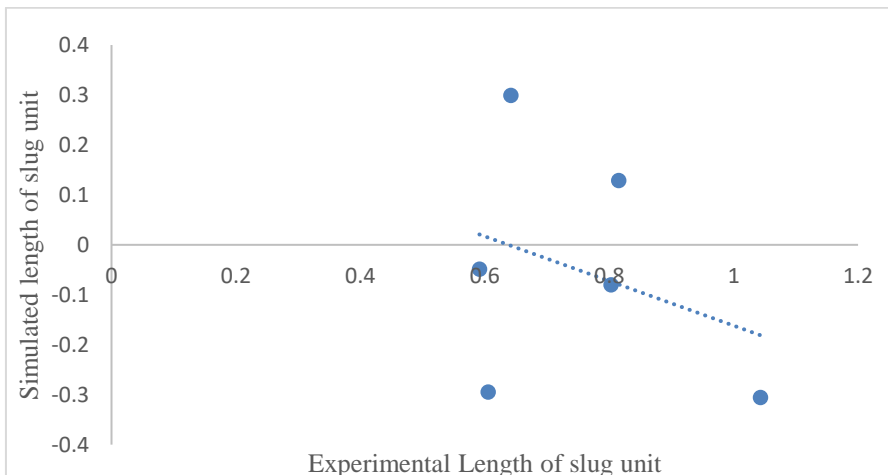


**Figure 4.38:** Cross plot of simulated vs experimental Length of slug unit at  $U_{sl} = 0.095$  m/s

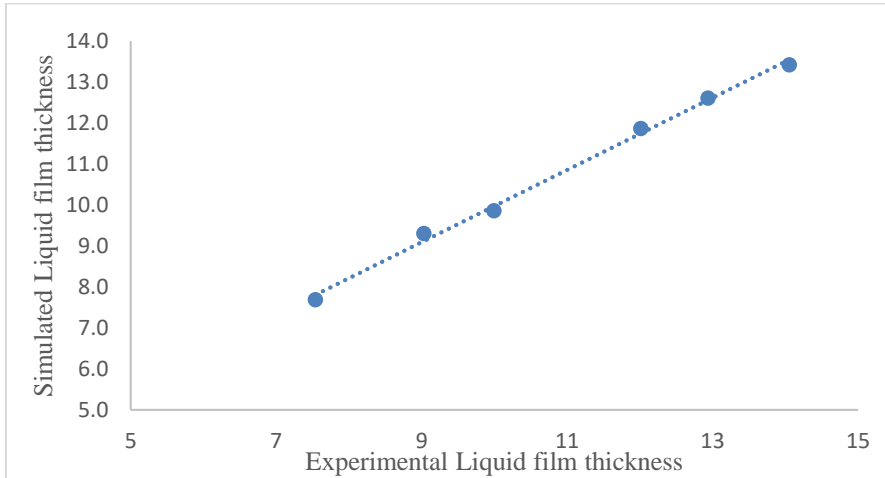


**Figure 4.39:** Cross plot of simulated vs experimental Liquid film thickness at  $U_{sl} = 0.095$  m/s

There were little correlation between experimental and simulated the length of slug unit this is due to the fact that it is dependent on mixture velocity and slug frequency, whose prediction has limitations from the model as seen in Figures 4.40. While a good fit between the experimental and very slight over predictions of liquid film thickness at Liquid superficial velocity of 0.142 m/s was observed as shown in Figure 4.41, this shows very good estimation can be gotten using the model.

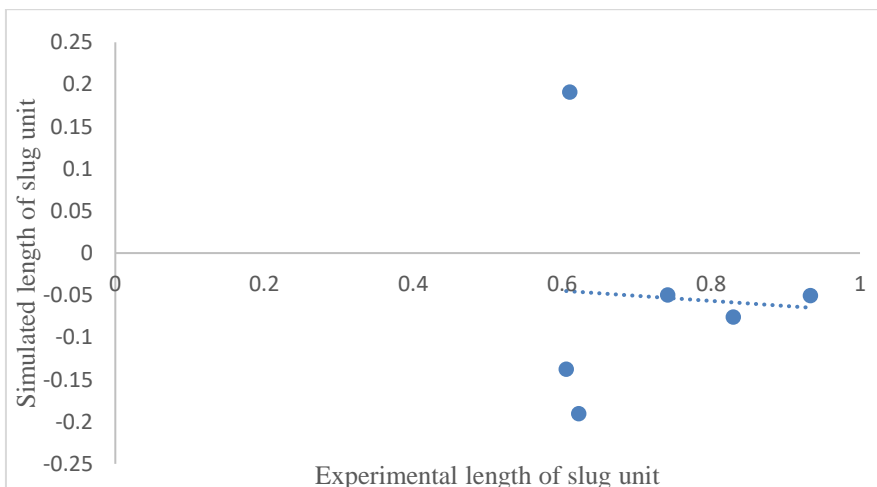


**Figure 4.40:** Cross plot of simulated vs experimental Length of slug unit at  $U_{sl} = 0.142$  m/s

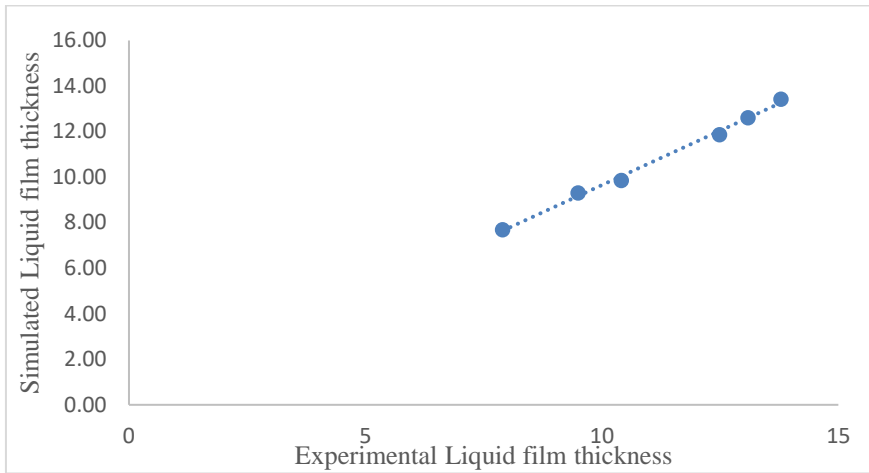


**Figure 4.41:** Cross plot of simulated vs experimental Liquid film thickness at  $U_{sl} = 0.142$  m/s

It can be deduced that little correlation between experimental and simulated the length of slug unit this is due to the fact that it is dependent on mixture velocity and slug frequency, whose prediction has limitations from the model as shown in Figures 4.42. While a good fit between the experimental and slight over predictions of liquid film thickness at Liquid superficial velocity of 0.284 m/s was observed and shown in Figure 4.43, this shows very good estimation can be gotten using the model.

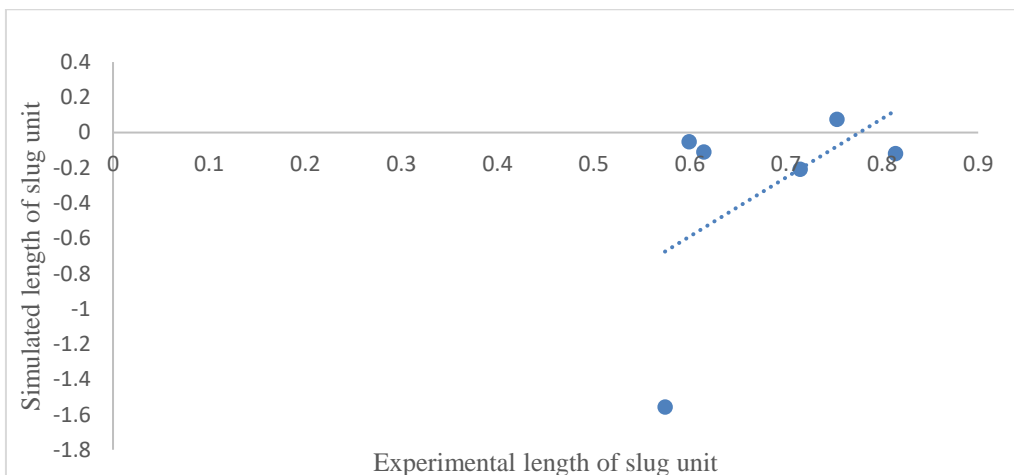


**Figure 4.42:** Cross plot of simulated vs experimental Length of slug unit at  $U_{sl} = 0.284$  m/s

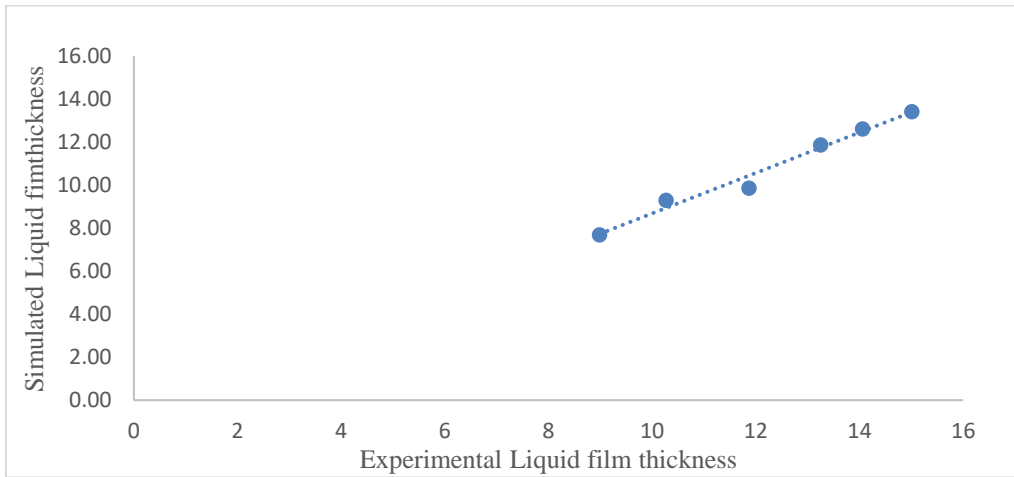


**Figure 4.43:** Cross plot of simulated vs experimental Liquid film thickness at  $U_{sl} = 0.284$  m/s

There were over predictions in length of slug unit this is due to the fact as the liquid velocity increased to 0.378 m/s from the model as shown in Figures 4.44. While a good fit between the experimental and slight over predictions of liquid film thickness at Liquid superficial velocity of 0.378 m/s was observed and shown in the cross plot in Figure 4.45, this shows very good estimation can be gotten using the model.

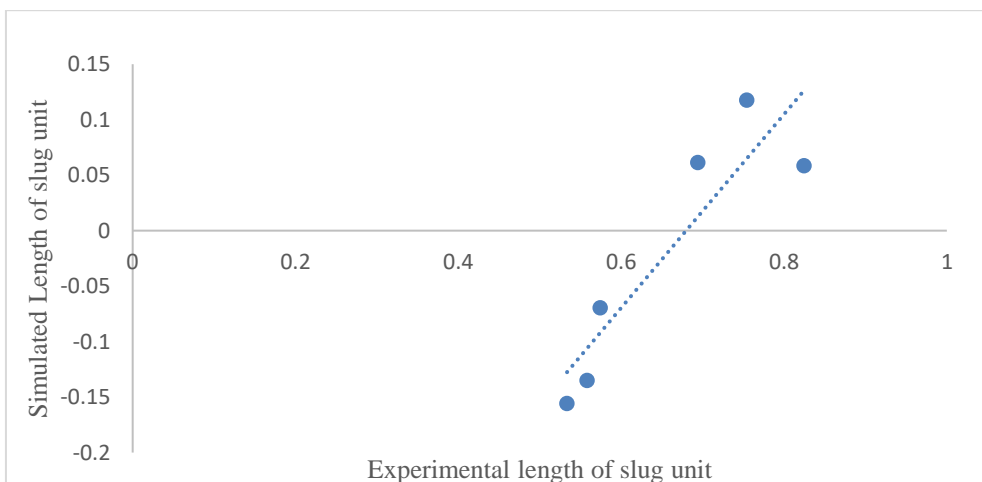


**Figure 4.44:** Cross plot of simulated vs experimental Length of slug unit at  $U_{sl} = 0.378$  m/s

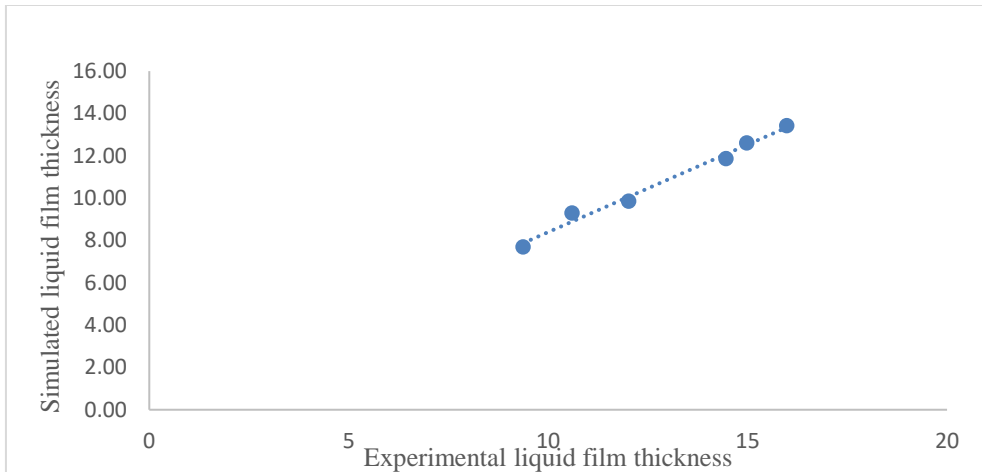


**Figure 4.45:** Cross plot of simulated vs experimental Liquid film thickness at  $U_{sl} = 0.378$  m/s

#### 4.4 The Correlation of Simulated and Experimental Liquid Hold-up at Varying

##### Viscosity

It has been deduced that structural (translational) velocity is affected by increase in the fluid viscosity. Al-kayiem *et al.*, (2017) carried out statistical assessment of slug body length and translational velocity using water as the liquid phase, they noted that for a fixed water velocity, the slug length and structural velocity increases with an increase in the superficial air velocity while the slug frequency decreased. Bendiksen *et al.*, (1984) utilized oil of viscosity ranging from 240–730 cP in a 0.057 m internal diameter horizontal pipe to study slug bubble velocity. The authors observed that liquid viscosity has a strong effect on bubble shape and velocity. This shows the machine learning model is good in estimating liquid hold-up, void fraction, and length of film thickness but has limitations in the slug frequency, length of slug unit and structural velocity.

The Figures 4.46 and 4.47 shows the random forest model tested with high viscosity multiphase data of 100 cP and 5000 cP. It is seen that the model gives a good plot at lower viscosity of 100 cP while it becomes less stable as the viscosity gets to 5000 cP. This follows the trend seen in Kora (2012).

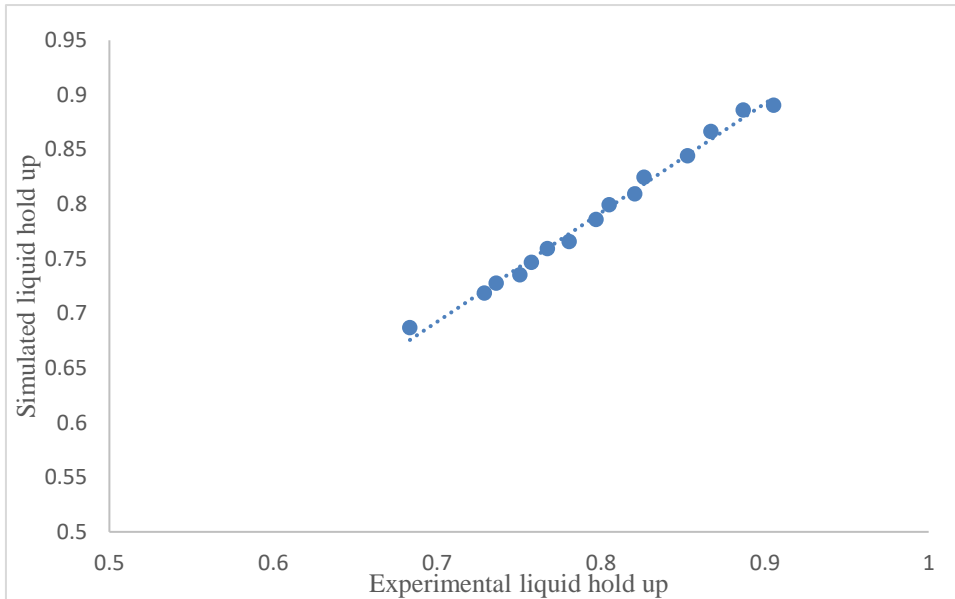


**Figure 4.46:** Cross plot of simulated vs experimental liquid hold up at viscosity = 100 cP

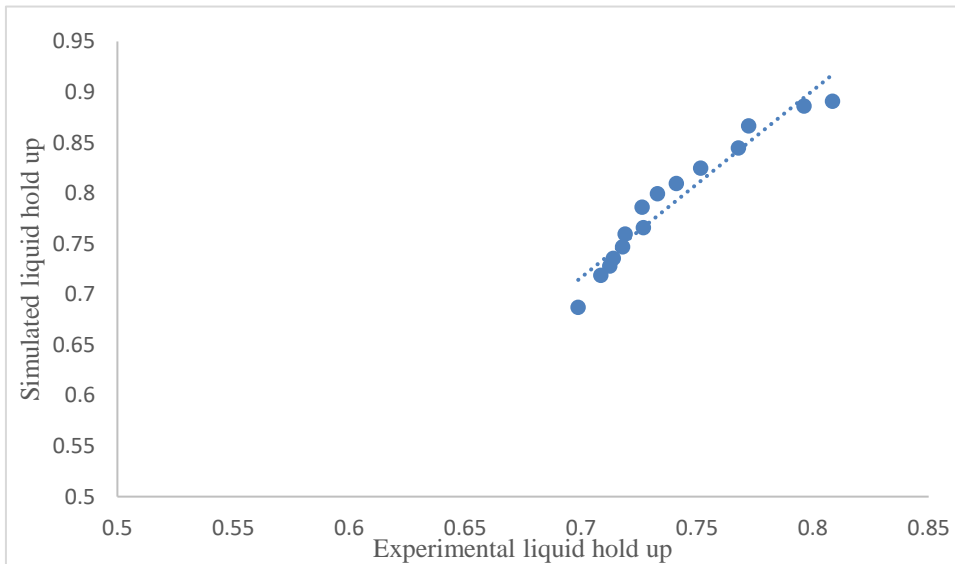


**Figure 4.47:** Cross plot of simulated vs experimental liquid hold up at viscosity = 5000 cP

#### 4.5 Performance Evaluation Mean Square Error

The results of the performance comparison of the matrix techniques are presented. The metrics for evaluating the performance of the techniques is based on the Mean Square Error (MSE), The comparative performance of the metrics form the basis for selecting the best performance evaluation technique used for testing the system. The results depict the minimum error technique as having the least values as compared with other techniques. These metrics is the measure of errors between the actual measurements and the simulated, thus the smaller the values, the better the performance.

The technique adopted Mean Squared Error (MSE) or mean squared deviation (MSD) of an estimator (of a procedure for estimating an unobserved quantity) measures the average of the squares of the errors that is, the average squared difference between the estimated values and what is estimated.

This is given as follows

$$MSE = \frac{1}{n} \sum_{i=1}^n (Y_i - Y_p)^2 \quad (3.0)$$

Let  $Y_i$  = value of Actual data

Let  $Y_p$  = value of data from the evolved technique(Predicted)

**MSE = 0.001984832 (0.2%)**

**Table 1.0: The matrix of values for the results obtained and Mean Squared Error = 0.001984832 (0.2 %)**

<b>S/N</b>	<b>H<sub>L</sub></b>	<b>H<sub>L</sub> Simulated</b>	<b>Squared Error</b>
1	0.785896	0.851135194331589	0.004256093
2	0.768684	0.851135194123256	0.006798253
3	0.569899	0.640851454112417	0.005034284
4	0.533710	0.611169074916500	0.005999871
5	0.519968	0.582884941959748	0.003958593
6	0.459412	0.501849199069167	0.001800892
7	0.393191	0.478255502997312	0.007235924
8	0.663012	0.640851454111820	0.000491103
9	0.623254	0.611169074918463	0.000146045
10	0.588582	0.582884941959809	0.000032453
11	0.507583	0.501849199070353	0.000032873
12	0.466540	0.478255502997312	0.000137251
13	0.399461	0.406455187217086	0.000048918
14	0.653691	0.640851454	0.000164862
15	0.628829	0.611169075	0.000311864
16	0.606551	0.582884941959809	0.000560063
17	0.52506	0.501849199	0.000538720
18	0.486545	0.478255502997312	0.000068723
19	0.416203	0.406455187217086	0.000095024

## CHAPTER FIVE

### 5.0 CONCLUSION AND RECOMMENDATIONS

#### 5.1 Conclusion

In this work, the experimental data obtained with a 67 mm diameter vertical pipe for air-silicone oil slug flow regime have been presented. Machine learning models developed and then used for prediction. Comparisons were made between the experimental and predicted data for liquid hold up, void fraction, structure velocity, slug frequency, length of slug unit, and liquid film thickness.

It can be concluded that:

1. The liquid hold up decreases with increasing gas superficial velocity at constant liquid superficial velocity as seen in Kong *et al.*, 2018, and Hernandez- Alvarado *et al.*, 2017.
2. The model generated showed a good fit of over 99 % in predicted slug flow parameters of liquid hold up, void fraction, and liquid film thickness under the flow conditions for the work.
3. The model showed high deviations in the slug frequency, length of slug unit, and structure velocity this could be attributed to data leakage in the machine learning model creation based on the flow parameters considered. This leads to limitation in using the model to predict the above slug flow parameters.
4. Viscosity has a significant effect on the prediction of the liquid hold up as over and under predictions were observed when the model was used to predict high viscosity of 5000 cP data. While at low viscosity of 100 cP, a perfect prediction was observed.

5. The Machine learning gives a very accurate prediction under the flow conditions and can be useful in multiphase flow predictions.

## **5.2 Recommendations**

Based on the results obtained and the conclusions of this study. The following recommendations are made:

1. The Machine learning random forest model for inclined and horizontal fluid flow can be generated and predicted to observe the predictability of the model.
2. More Multiphase flow parameters can be generated from the models in slug flow as well as other flow patterns to see the predictability in varying flow conditions.
3. Structure velocity, slug frequency and length of slug unit models can be further generated by considering liquid viscosity and pressure data.

## **5.3 Contribution to Knowledge**

1. A Random forest-based model was developed in machine learning to predict Liquid holdup and slug flow characteristics in an Air-Silicone Oil 67mm diameter and 6m long vertical pipe. The time series data comprises of superficial velocity ranges of gas and liquid obtained from the ECT were 0.047 – 4.727m/s and 0.05 – 0.284m/s respectively. The predicted liquid holdup had a mean square error of 0.2%.
2. The study shows the developed random-forest based model has a high degree of accuracy and useful in the handling of slug flow in multiphase flow however limitations were seen in prediction of some slug flow characteristics namely structure velocity, length of slug unit, and slug frequency while length of film thickness and void fraction had a perfect fit using the model.

3. The study also shows the effectiveness of machine learning in handling complex data in design and handling of process operation for greater efficiency. This is useful particularly when mathematical model could not describe the process due to complexity of data.

## REFERENCES

- Abdulkadir, M., Hernandez-Perez, V., Lo, S., Lowndes, I. S., & Azzopardi, B. J. (2015). Comparison of experimental and computational fluid dynamics (CFD) studies of slug flow in a vertical riser, *experimental thermal and fluid science*, 68, 468-483, [DOI:10.1016/j.expthermflusci.2015.06.004](https://doi.org/10.1016/j.expthermflusci.2015.06.004).
- Abdulkadir, M., Hernandez-Perez, V., Sharaf, S., Lowndes, I. S. & Azzopardi, B. J. (2015). Phase distribution of an air-silicone oil mixture in a vertical riser”, 7th international conference on heat transfer, fluid mechanics and thermodynamics, Antalya, Turkey.
- Abdulkadir, M., Hernandez-Perez, V., Lowndes, I. S., Azzopardi, B. J., Dzomeku, S. (2014). Experimental study of the hydrodynamic behaviour of slug flow in a vertical riser, *Chemical Engineering Science*, 106, 60-75, [DOI:10.1016/j.ces.2013.11.021](https://doi.org/10.1016/j.ces.2013.11.021).
- Abdulkadir, M., Zhao, D., Sharaf, S., Abdulkareem, L., Lowndes, I. S., Azzopardi, B. J. (2011). Interrogating the effect of 90° bends on air–silicone oil flows using advanced instrumentation, *Chemical Engineering Science*, 66, 2453-2467, [DOI:10.1016/j.ces.2011.03.006](https://doi.org/10.1016/j.ces.2011.03.006).
- Abdulkadir, M., Zhao, D., Sharaf, S., Abdulkareem, L. S., Lowndes, I. S., Azzopardi, B. J., (2010). Interrogating the effect of bends on gas-liquid flow using advanced instrumentation, ICMF 2010, 7th International Conference on Multiphase Flow, Tampa, FL, USA.
- Abiodun, O. I., Jantan, A., Omolara, A. E., Dada, K. V., Mohamed, N. A., & Arshad, H. (2018). State-of-the-art in artificial neural network applications: A survey. *Heliyon*, 4(11), e00938. [DOI:10.1016/j.heliyon.2018.e00938](https://doi.org/10.1016/j.heliyon.2018.e00938).
- Al-Azzawi, M., Mjalli, F. S., Husain, A., Al-Dahhan, M. (2021). A Review on the hydrodynamics of the Liquid–Liquid two-phase flow in the microchannels. *Industrial & Engineering Chemistry Research* 2021, 60, 5049–5075.
- Al-Kayiem, H. H., Mohmmed, A. O., Al-Hashimy, Z. I., Time, R. W. (2017). Statistical assessment of experimental observation on the slug body length and slug translational velocity in a horizontal pipe. *International Journal of Heat and Mass Transfer*, 105, 252–260.
- Almalki, N., & Ahmed, W. H. (2019). Experimental investigation of pressure and void fraction changes for two-phase flow through flow-restricting orifices. *Journal of WIT Transactions on Engineering Sciences*, 123, (159-168).
- Asikolaye, N. O. (2019). Analysis of horizontal air-silicone oil plug-to-slug transition flow. Retrieved from <http://repository.aust.edu.ng/xmlui/handle/123456789/4929>.

- Azzopardi, B. J., Hernandez Perez, V., Kaji, R., Da Silva, M. J., Beyer, M., & Hampel, U. (2008). Wire mesh sensor studies in a vertical pipe, HEAT 2008, Fifth International Conference on Multiphase Systems, Bialystok, Poland.
- Barnea, D., Shoham, O., Taitel, Y., & Dukler, A. E. (1980). Flow pattern transition for gas-liquid flow in horizontal and inclined pipes. Comparison of experimental data with theory. *International Journal of Multiphase Flow* 6(3): 217-225. DOI:10.1016/0301-9322(-80)90012-9.
- Bendiksen, K. H. (1984). An experimental investigation of the motion of long bubbles in inclined tubes. *International Journal of Multiphase Flow* 10(4), 467–483
- Brennen, C. E. (2005). Fundamentals of multiphase flows. California Institute of Technology. Cambridge University Press. ISBN 0521 848040.
- Cai, B., Guo, D. X., & Jing, F. W. (2016). Study on gas-liquid two-phase flow patterns and pressure drop in a helical channel with complex section. In proceedings of the 23rd International Compressor Engineering Conference, West Lafayette, IN, USA, 11–14 July 2016.
- Carpintero, E. (2009). Experimental Investigation of Developing Plug and Slug Flows. 138. Retrieved from [http://nbn-resolving.de/urn/resolver.pl?urn:nbn:de:bvb:91-diss\\_20090825-738028-1-2](http://nbn-resolving.de/urn/resolver.pl?urn:nbn:de:bvb:91-diss_20090825-738028-1-2).
- Choi, J., Pereyra, E., & Sarica, C. (2012). An efficient drift-flux closure relationship to estimate liquid holdups of gas–liquid two-phase flow in pipes. *Energies* 5(12), 5294–5306.
- Daev, Z. A., & Kairakbaev, A. K. (2017). Measurement of the flow rate of liquids and gases by means of variable pressure drop flow meters with flow straighteners. *International Journal Measurement Science and Technology*. 2017, 59, 1170–1174. DOI:10.1007/s11018-017-1110-x.
- Davies, R. M. & Taylor, G. I. (1950). The mechanics of large bubbles rising through extended liquids and through liquids in tubes. *Journal of Proceedings of the Royal Society of London, Series. A Mathematical and Physical Sciences* 200(1062), 375. DOI:10.1098/rspa.1950.0023
- Ehinmowo, A. B., Ogunbiyi, A.T., Orodu, O. D., Aribike, D. S., & Denloye, A. O. (2016). Experimental investigation of hydrodynamic slug flow in pipeline-riser systems. *International Journal of Applied Engineering Research*, 11(22), 10794-10799
- El-Abbasy, M., Senouci, A., Zayed, T., Mirahadi, F., & Parvizsedghy, L. (2014). Condition prediction models for oil and gas pipelines using regression analysis. *Journal of*

*Construction Engineering and Management* 140. 04014013. 10.1061/ (ASCE) CO. 1943-7862.0000838.

- Fabre, A., & Line, A. (2003). Modeling of two-phase slug flow. *Annual Review of Fluid Mechanics* 24(1), 21–46.
- Fadare, D. A. & Ofidhe, U. I. (2009). Artificial neural network model for prediction of friction factor in pipe flow. *Journal of Applied Sciences* 5, 662–670.
- Felizola, H. (1992). Slug flow in extended reach directional wells. M.S. Thesis, the University of Tulsa, Tulsa, OK
- Ganat, T., & Hrairi, M. (2019). Effect of flow patterns on two-phase flow rate in vertical pipes. *Journal of Advanced Research in Fluid Mechanics and Thermal Sciences* 55. 150-160.
- Griffith, P. (1962). Two-phase flow in pipes. in special summer program; Massachusetts Institute of Technology: Cambridge, MA, USA.
- Gokcal, B., Wang, Q., & Zhang, H. Q. (2008). Effects of high oil viscosity on oil/gas flow behavior in horizontal pipes. *SPE Projects, Facilities, and Construction*. 3(2), 1–11
- Gregory, G.A., Nicholson, M. K., & Aziz, K. (1978): Correlation of the liquid volume fraction in the slug for horizontal gas–liquid slug flow. *International Journal of Multiphase Flow* 4(1), 33–39.
- Hernandez-Alvarado, F., Kalaga, D. V., Turney, D., Banerjee, S., Joshi, J. B., & Kawaji, M. (2017). Void fraction, bubble size and interfacial area measurements in cocurrent downflow bubble column reactor with microbubble dispersion. *Journal of Chemical Engineering Science* 168(May), 403–413. [DOI:10.1016/j.ces.2017.05.006](https://doi.org/10.1016/j.ces.2017.05.006).
- Hernandez-Perez, V. (2007). Gas-liquid two-phase flow in inclined pipes, a PhD thesis, University of Nottingham, United Kingdom.
- Hewitt, G. F. (1982). Flow regimes handbook of multiphase systems (ed: G. Hetsroni). McGraw-Hill Book Co.
- Jamshed, S. (2015). Introduction to CFD using HPC for computational fluid dynamics. a guide to high performance computing for CFD engineers [DOI:10.1016/B978-0-12-801567-4.00001-5](https://doi.org/10.1016/B978-0-12-801567-4.00001-5).
- Jiang, J. Z., Zhang, W. M., Wang, Z. M. (2011). Research progress in pressure-drop theories of gas-liquid two-phase pipe flow. In proceedings of the china international oil & gas Pi (CIPC 2011), Langfang, China, 5 September 2011.

- Jyothi, P. N. S. & Yamaganti, R. (2019). A review on python for data science, machine learning and IOT. *International Journal of Scientific & Engineering Research* Volume 10.
- Kaul, A. (1996). Study of slug flow characteristics and performance of corrosion inhibitors, in multiphase flow, in horizontal oil and gas pipelines (MSc Theses), Ohio University.
- Kong, R., Rau, A., Kim, S., Bajorek, S., Tien, K., & Hoxie, C. (2018). Experimental study of horizontal air-water plug-to-slug transition flow in different pipe sizes. *International Journal of Heat and Mass Transfer* 123, 1005–1020. DOI:10.1016/j.ijheatmasstransfer.2018.03.027.
- Kora, C., Sarica, C., & Zhang, H. Q. (2011). Effects of high oil viscosity on slug liquid holdup in horizontal pipes. *SPE Projects, Facilities, and Construction*. 4(2), 32–40.
- Kristian, K. (2018). Machine learning and artificial intelligence: two fellow travelers on the quest for intelligent behavior in machines. *Frontiers in Big Data*. 10.3389/fdata.2018.00006.
- Kwatia, C. A. (2016). Investigating the behaviour of air-silicone oil flows in vertical and horizontal pipes for effective gas-liquid transport. Retrieved from <https://repository.aust.edu.ng/xmlui/handle/123456789/525>
- Lakehal, D. (2013). Advanced simulation of transient multiphase flow & flow assurance in the oil & gas industry. *Canadian Journal of Chemical Engineering* 91: 1201-1214. DOI: 10.1002/cjce.21828
- Manera, A., Ozar, B., Sidharth, P., Ishii, M., & Prasser, H. M. (2009). Comparison between wire-mesh sensors and conductive needle-probes for measurements of two-phase flow parameters. *Journal of Nuclear Engineering and Design* 239. 1718-1724. 10.1016/j.nucengdes.2008.06.015.
- Mijwel, M. (2018). Artificial neural networks advantages and disadvantages. Reviewed by Springer Nature. Retrieved from <https://www.linkedin.com/pulse/artificial-neural-networks-advantages-disadvantages-maad-m-mijwel/>
- Monni, G., De Salve, M., Panella, B. (2014). Horizontal two-phase flow pattern recognition, *Journal of Experimental Thermal and Fluid Science* 59, 213-221. DOI:10.1016/j.expthermflusci.2014.04.010.
- Nadler, M., & Mewes, D. (1995). Effects of the liquid viscosity on the phase distributions in horizontal gas–liquid slug flow. *International Journal of Multiphase Flow*. 21(2), 253–266.

- Nicklin, D. J. (1962). Two-phase flow in vertical tubes. *Journal of Transactions of the Institution of Chemical Engineers* 1962, 40, 61–68.
- Nitaware, R. (2019). Basic fundamental of python programming language and the bright future. *A Peer-Reviewed Journal About VIII*. 71-76.
- Oliveira, J. L. G., Passos, J. C., Verschaeren, R., & Van der Geld, C. (2009). Mass flow rate measurements in gas-liquid flows by means of a venturi or orifice plate coupled to a void fraction sensor. *Journal of Experimental Thermal and Fluid Science* 2009, 33, 253–260. [DOI:10.1016/j.expthermflusci.2008.08.008](https://doi.org/10.1016/j.expthermflusci.2008.08.008).
- Oteng, B. (2014). Effect of pipe inclination angle on gas-liquid flow using electrical capacitance tomography (ECT) data.
- Ren, G., Ge, D., Li, P., Chen, X., Zhang, X., Lu, X., Sun, K., Fang, R., Mi, L., Su, F. (2021). The flow pattern transition and water holdup of gas-liquid flow in the horizontal and vertical sections of a continuous transportation pipe. *water*. 2021; 13(15):2077. [DOI:10.3390/w13152077](https://doi.org/10.3390/w13152077).
- Saeb, M. B., Philip, D. M., David, C. C., & Ali, J. (2015). Modeling friction factor in pipeline flow using a GMDH (Group Method of Data Handling)-type neural network. *Journal of Cogent Engineering* 2. [DOI:10.1080/23311916.2015.1056929](https://doi.org/10.1080/23311916.2015.1056929).
- Shaban, H., & Tavoularis, S. (2014). Identification of flow regime in vertical upward air-water pipe flow using differential pressure signals and elastic maps. *International Journal Multiphase Flow* 2014, 61, 62–72. [DOI:10.1016/j.ijmultiphaseflow.2014.01.009](https://doi.org/10.1016/j.ijmultiphaseflow.2014.01.009).
- Shaikh, A. & Al-Dahhan, M. (2007). A review on flow regime transition in bubble columns. *International Journal of Chemical Reactor Engineering* 5. 1. [DOI:10.2202/1542-6580.1368](https://doi.org/10.2202/1542-6580.1368).
- Shannak, B. A. (2008). Frictional pressure drops of gas liquid two-phase flow in pipes. *Journal of Nuclear Engineering and Design* 238, 3277–3284.
- Shen, X., Mishima, K., and Nakamura, H. (2004). Two-phase distribution in a vertical large diameter pipe, *International Journal Heat and Mass Transfer* 48, 211-22
- Taitel, Y., & Dukler, A. E. (1976). A model for predicting flow regime transitions in horizontal and near horizontal gas-liquid flow. *AIChE J.*, 22, 47-55.
- Tek, M. R. (1961). Multiphase flow of water, oil and natural gas through vertical flow strings." *Journal of Petroleum Technology* 13 (1961): 1029–1036. [DOI:10.2118/1657-G-PA](https://doi.org/10.2118/1657-G-PA).

- Thome J. R. & El Hajal, J. (2010). Two-phase flow pattern map for evaporation in horizontal tubes: latest version, *Journal of Heat Transfer Engineering*, 24:6, 3-10, [DOI:10.1080/714044410](https://doi.org/10.1080/714044410)
- Wang, H., Zhang, M., Yang, Y. (2020). Machine learning for multiphase flowrate estimation with time series sensing data. 10–12. [DOI:10.1016/j.measen.2020.100025](https://doi.org/10.1016/j.measen.2020.100025).
- Xiao, J. J. (2011). A Comprehensive mechanistic model for two-phase flow in pipelines. M.S. Thesis, U. of Tulsa, Tulsa, OK
- Xu, Y., Fang, X. D., Su, X. H., Zhou, Z. R., & Chen, W. W. (2012). Evaluation of frictional pressure drop correlations for two-phase flow in pipes. *Journal Nuclear Engineering and Design* 253, 86–97. [DOI:10.1016/j.nucengdes.2012.08.007](https://doi.org/10.1016/j.nucengdes.2012.08.007).